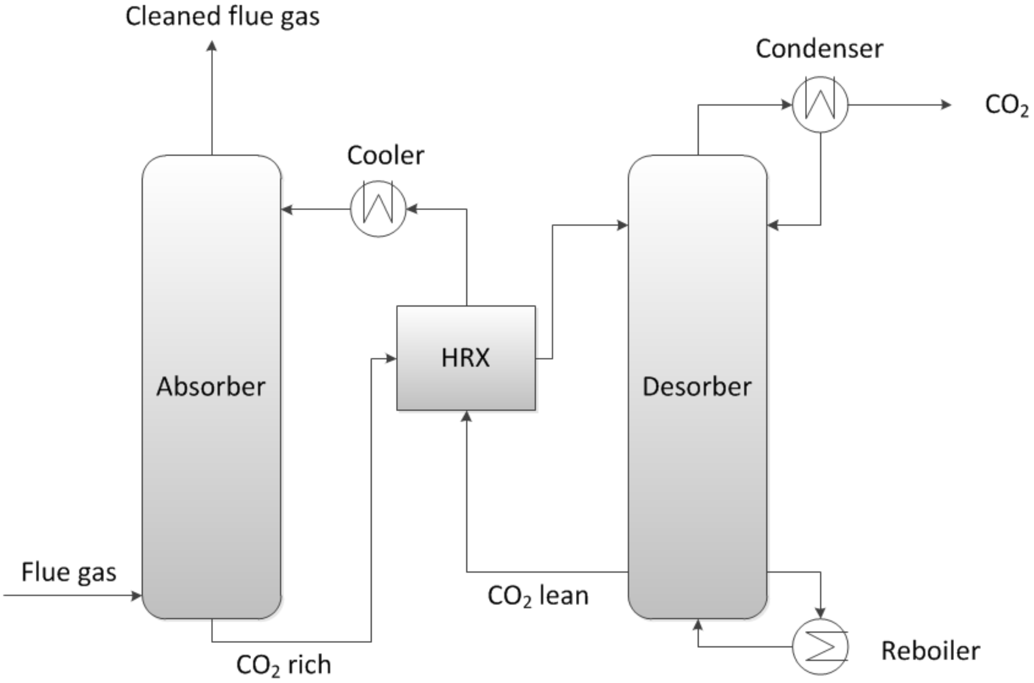
Cleaned flue gas
Condenser
CO_2
Cooler
Absorber
HRX
Desorber
Flue gas
CO_2 lean
CO_2 rich
Reboiler

Transient behaviour of post-combustion CO_2 capture with MEA in coal fired power plants

Master of Science Thesis [Sustainable Energy Systems]

SÓLEY EMILSDÓTTIR
STEFANÍA ÓSK GARÐARSDÓTTIR

Department of Energy and Environment
Division of Energy Technology
CHALMERS UNIVERSITY OF TECHNOLOGY
Gothenburg, Sweden, 2012
Report No. T2012-375

REPORT NO. T2012-375

Transient behaviour of post-combustion CO_2 capture with MEA

Sóley Emilsdóttir
Stefanía Ósk Garðarsdóttir

Supervisors: Ph.D. Fredrik Normann
Ph.D. Katrin Prölß
Ph.D. Jens Pålsson

Examiner: Docent Klas Andersson

Department of Energy an Environment
CHALMERS UNIVERSITY OF TECHNOLOGY
Gothenburg, Sweden, 2012

Transient behaviour of post-combustion CO_2 capture
in power plants

SÓLEY EMILSDÓTTIR
STEFANÍA ÓSK GARÐARSDÓTTIR

© SÓLEY EMILSDÓTTIR & STEFANÍA ÓSK GARÐARSDÓTTIR,
2012.

Technical report NO. T2012-375
Department of Energy and Environment
CHALMERS UNIVERSITY OF TECHNOLOGY
SE-412 96 Gothenburg
Sweden
Telephone +46 (0)31 772 1000

Chalmers Reproservice
Gothenburg, Sweden 2012

Abstract

CO_2 emissions are recognized as a large contributing factor to global warming and climate change. Post-combustion CO_2 capture has received significant attention as a possible near term option for reducing CO_2 emissions from coal fired power plants as emissions from such plants are one of the major anthropogenic sources of CO_2 in the world. Increased requirements for load flexibility in coal fired power plants make dynamic analysis of the capture process necessary. This thesis takes part in the development of a dynamic model of a CO_2 absorption process with monoethanolamine (MEA) by constructing a reboiler model and by implementing strategies for process control. The model is applied to investigate the transient behaviour of the absorption system during and after load changes.

The results show that the model gives a good understanding of the dynamic behaviour of the capture process. It is shown that the liquid-to-gas (L/G) ratio is more important than the actual flow rates for maintaining desired capture efficiency when the size of the system is not limiting the process. Results from load variations show that implementation of control strategies lowers the energy demand of the process considerably and this becomes clearer with larger load variations. It takes the system longer time to reach steady state with larger load variations, or 60 minutes at most. It takes the system around 20 seconds to respond to the load variations in all cases studied. The responses are generally smooth with little or no fluctuations and small overshoots. The fast system response and relatively small fluctuations and overshoots attained will facilitate integration with a power plant.

Keywords: Post combustion, CO_2 capture, chemical absorption, MEA, dynamic modelling.

Contents

Abstract I

Contents III

Preface V

Abbreviations and symbols VII

1 Introduction 1

1.1 Background 1

1.2 Aim and scope 1

2 Theory 3

2.1 Post-combustion capture with MEA 3

2.2 Dynamic modelling of post-combustion units 4

3 Method 7

3.1 Modelling tool 7

3.2 Assumptions and limitations 7

3.3 Effects of load changes 7

4 Model 9

4.1 Model review 9

4.2 Discretization 13

4.3 Development of reboiler model 15

4.4 Development of control strategies 17

4.4.1 Control strategies for scenario 1 – Part load operation 18

4.4.2 Control strategies for scenario 2 – Limited steam availability 19

5 Results – Model development 21

5.1 Parametric study - Tuning of system 21

5.2 Parametric study - Effect of geometrical design parameters 22

5.3 Impact of L/G ratio on capture efficiency 24

5.4 Selection of reboiler control strategy 25

6 Results – Effects of load changes 27

6.1 Scenario 1 – Part load operation 27

6.1.1 Discussion 29

6.2 Scenario 2 – Peak demand 30

6.2.1 Discussion 32

7 Conclusions 35

8 Future work 37

9 References 39

10 Appendix A – Scenario 1 41
10.1 Load reduction from full load down to 60% load 41
10.2 Load reduction from full load down to 40% load 42
11 Appendix B – Scenario 2 43
11.1 Steam flow reduction of 30% 43
11.2 Steam flow reduction of 50% 44

Preface

In this master’s thesis, transient behaviour of post-combustion CO_2 capture system with MEA is investigated in collaboration with Modelon.

We would like to acknowledge and thank our supervisors at Modelon, Jens Pålsson and Katrin Prölss, for their assistance and Katrin especially for being able to answer every single question and thereby helping us gaining the understanding of the absorption process and the model we have today.

Many thanks to our supervisor at Chalmers, Fredrik Normann, for his greatly appreciated help and instructions during the thesis work. We would also like to thank our opponents, Marika Thureson and Åsa Leander, for their support and suggestions of improvements.

We would also like to thank Landsvirkjun, which partly funded this thesis work.

Finally, we especially like to thank our examiner, Klas Andersson, for making time for us in his extremely busy schedule and for his guidance.

Sóley Emilsdóttir & Stefanía Ósk Garðarsdóttir

Abbreviations and symbols

Abbreviations

CCS	Carbon Capture and Storage
L/G	Liquid-to-Gas
MEA	Monoethanolamine
NJV	Nordjyllandsværket

Greek symbols

Symbol	Meaning	Unit
α	Heat transfer coefficient	W/(m^2·K)
λ	Fluid conductivity	W/(m·K)

Latin symbols

A	Heat transfer area	m^2
A_{cross}	Absorber cross sectional area	m^2
A_{liq}	Heat transfer area of condensate	m^2
A_{steam}	Heat transfer area of condensing steam	m^2
A_{tot}	Total heat transfer area of tubes	m^2
d_{hyd}	Hydraulic diameter of a pipe	m
$\dot{m}_{CO_2}$	Mass flow rate of CO_2 from NJV	kg/s
Nu_{mean}	Mean Nusselt number	-
$\dot{n}_{CO_2}$	Molar flow rate of CO_2	mol/s
$\dot{n}_g$	Molar flow rate of gas	mol/s
$\dot{n}_l$	Molar flow rate of liquid	mol/s
$\dot{n}_{MEA}$	Molar flow rate of MEA	mol/s
n_{cap}	Capture efficiency	-
$\dot{Q}_{conv}$	Heat transferred by convection	W
$\dot{Q}_{process}$	Heat demand of the capture process	W
$q_{reboiler}$	Reboiler duty	J/kg CO_2 captured
T_c	Temperature of condensate	K
T_s	Temperature of solution	K
t_{res}	Residence time	s
V_{fluid}	Volume of fluid	m^3
$\dot{V}_{fluid}$	Fluid volume flow rate	m^3/s
$\dot{V}_g$	Gas volume flow rate	m^3/s
v_s	Superficial gas velocity	m/s
y	Relative level of condensate	-

1 Introduction

1.1 Background

CO_2 emissions are recognized as a large contributing factor to global warming and climate change. At present, governments, industries and society are looking for solutions to minimize the effect on the ecosystem for future generations. The long term goal is the complete replacement of fossil fuels with renewable energy sources. This will, however, not happen overnight, especially as the use of fossil fuels is still increasing [1]. In the meantime, effective CO_2 emission reduction strategies are required such as Carbon Capture and Storage (CCS). CCS is a process in which CO_2 is separated from the fuel before combustion or the flue gas stream, normally generated by combustion of fossil fuels. The relatively pure CO_2 stream is then compressed, transported and stored in such way that it is not released into the atmosphere. Possible storage sites are for example in deep geological formations or deep in the ocean.

Three major carbon capture technologies exist today: post-combustion, pre-combustion and oxy-fuel combustion [2]. This work investigates post-combustion. Post-combustion CO_2 capture has received significant attention as a possible near term option for reducing CO_2 emissions from coal fired power plants as emissions from such plants are one of the major anthropogenic sources of CO_2 in the world [3]. One of the advantages of post-combustion capture is that it may be retrofitted to existing processes as an "end-of-pipe" solution. This makes implementation of post-combustion CO_2 capture to existing infrastructure easier and less expensive than the two other alternatives. Post-combustion capture requires energy in the form of heat, which is usually taken from the steam cycle of the power plant. This has a negative impact on the power plant performance and it is important to minimize the energy demand of the process.

At present, the requirements of load flexibility are increasing in thermal power plants. The main reason is that more electricity is produced by intermittent energy sources, which requires regulating power from base load power plants [4]. To make CCS implementations economically feasible, the process has to be able to respond well to load changes without severe consequences for plant performance. It is, thus, of great importance to investigate the transient behaviour of the capture process.

1.2 Aim and scope

The aim of this thesis may be divided into two parts. The overall aim of the first part is to extend an existing dynamic model of a post-combustion capture process, which may be integrated with a CO_2 transportation network and a dynamic power plant model including flue gas system and a steam cycle. This thesis contributes to the model by development of a reboiler model that may be integrated with a steam cycle and by implementation of control strategies which makes it possible to control important variables in the capture process. In order to investigate the effect of load changes, several closed loop controllers are developed to control design variables such as capture efficiency and energy consumption. In addition, impact of the L/G ratio, which is the ratio between the liquid and gas in the absorber, on the capture efficiency is studied.

The second part investigates the transient behaviour of post-combustion CO_2 capture with MEA during load change in coal fired power plants. Coal fired power plants operate at different loads, which has a direct influence on the amount of flue gas generated and on the amount of steam produced for the steam cycle. One scenario studies how the capture process responds to reduction in power plant load and how long it takes for the system to reach steady state. Another scenario studies how changes in steam availability affect the process. The focus is on system dynamics of the process and the conclusions are generally applicable to MEA post-combustion capture systems.

2 Theory

The theory chapter includes background information to the thesis. It also reviews the research performed on process simulations of MEA post-combustion capture.

2.1 Post-combustion capture with MEA

CO_2 capture with MEA has been used for decades in the gas processing industry, for example in enhanced oil recovery or for gas sweetening in refineries [5]. Today this technology is being studied and tested as a potential CO_2 capture method for industries emitting CO_2, such as coal fired power plants. A simplified process scheme of the MEA post-combustion capture system is seen in Figure 2-1. Flue gas containing CO_2 enters the bottom of the absorber. At the top of the absorber the solvent, usually around 30 wt% MEA in water [6], enters and flows in the opposite direction to the flue gas. The solvent reacts with CO_2 and separates it from the flue gas stream. The absorption takes place close to atmospheric pressure and at a temperature between 40 and 60°C [6]. The remaining flue gas, mainly consisting of N_2, is released into the atmosphere. The CO_2 rich solvent enters a heat exchanger in order to recover heat from the CO_2 lean solvent stream before entering the desorber where heat is added to separate the CO_2 from the solvent. The separation of CO_2 in the desorber takes place at 1.5 to 2 bar and 100 to120°C [6]. The solvent leaves the desorber CO_2-lean and is cooled before it is reused in the absorber. After leaving the desorber, the almost pure CO_2 stream passes through a condenser to reduce the water content [7]. Finally, the relatively pure CO_2 stream is compressed and prepared for transport and storage. The heat consumption of the process is considerable or generally from 3.5 to 5 MJ/kg CO_2 captured [8] and the capture efficiency of the process can reach up to 95% [9].

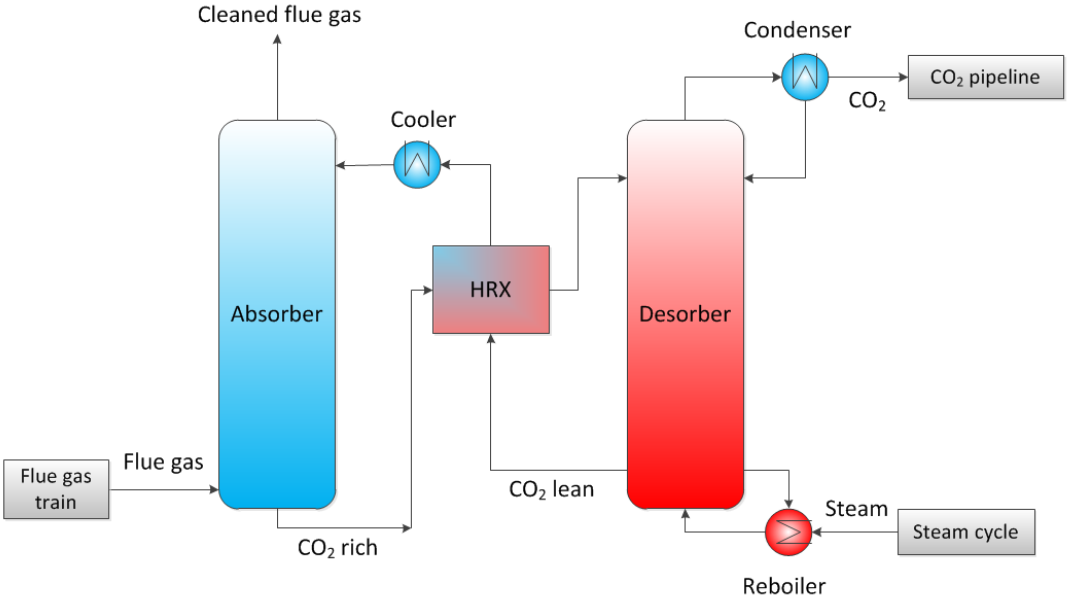

Figure 2-1: A simplified flow diagram of a chemical absorption process. The grey boxes represent the connected processes.

2.2 Dynamic modelling of post-combustion units

In the literature, two approaches are used to model the absorber and desorber in dynamic modelling: equilibrium-based and rate-based [10]. In both approaches the absorber and desorber are divided into several theoretical stages which are connected through mass and energy balance equations [11]. In the former approach the gas and liquid phases are assumed to reach chemical and thermodynamic equilibrium at each theoretical stage, which is not always the case due to too slow reactions or mass transfer. The latter approach considers the rate of mass transfer and in some cases the rate of chemical reactions, and is therefore more complex. Both the equilibrium-based and rate-based approaches can be used with different complexity.

Figure 2-2 summarizes the different types of modelling approaches. Models 1 and 2 in Figure 2-2 are both equilibrium-based. Model 1 assumes reaction equilibrium, that is, fast reactions relative to mass transfer, whereas model 2 accounts for reaction kinetics in the bulk phase. Models 3, 4 and 5 are rate-based. The mass transfer may be described with the two-film theory which assumes that the liquid and gas phases consist of bulk and film regions and an interface between the two phases where the mass transfer through the interface is driven by a concentration and pressure gradients existing in the film. Model 3 assumes chemical reactions at equilibrium. Model 4 includes reaction kinetics in the bulk and uses enhancement factor to describe the influence of reaction on the mass transfer in the liquid film. Model 5 is the most complex model as it includes mass transfer resistances, electrolyte thermodynamics and the reaction system in the liquid film and bulk [10]. The accuracy of the different levels of models depends on the application.

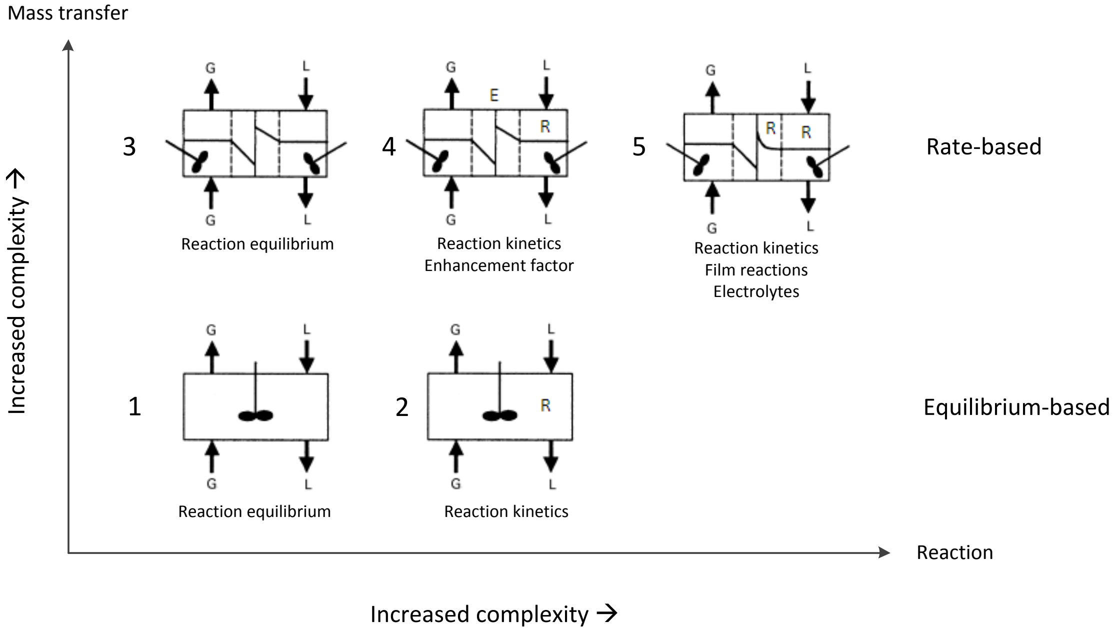
Mass transfer
Increased complexity →
3
4
5
G
L
E
R
Rate-based
Reaction equilibrium
Reaction kinetics
Enhancement factor
Reaction kinetics
Film reactions
Electrolytes
1
2
Equilibrium-based
Reaction equilibrium
Reaction kinetics
Reaction
Increased complexity →

Figure 2-2: Different levels of complexity for modelling of absorption processes [27].

Numerous steady-state analyses of the post-combustion capture process have been carried out and published, however limited work has been carried out regarding the dynamic behaviour of the process [10]. Steady-state analysis can give a good understanding of the process at design conditions, but does not reflect the transient behaviour of plant operation. The dynamic behaviour of the two major components of the post-combustion CO_2 capture process, the absorber and the desorber, has been studied by a number of researchers [12-16]. However, the modelling and simulation of those components has most often been done separately instead of modelling the whole capture process. Below is a short listing of the main research that has been performed on dynamic modelling of CO_2 capture with MEA and the modelling approaches used.

In Ref. [12] a dynamic model of the absorber is developed according to model 3 in Figure 2-1. The focus of this study is to compare equilibrium- and rate-based modelling approaches and to study the dynamic behaviour of the system when operating at part load. The main conclusions are that 1) the rate-based model is better than the equilibrium-based model at predicting the behaviour of the chemical absorption process, and 2) the performance at part load can be maintained if the ratio between the flue gases and the lean solvent entering the absorber is held constant. In Ref. [13] a dynamic model of the absorber is also constructed but according to model 4. The main focus is on investigating the transient behaviour of two main scenarios: start-up and load reduction. Also, issues regarding load changes in a power plant upstream of the process are discussed. The main results show that the absorber model can give a good understanding of the dynamic behaviour of the process but a model of the whole capture process is needed to evaluate all operation challenges. In Ref. [14] dynamic models of both the absorber and desorber are constructed separately according to model 3. The main results show that 1) the absorber performance is sensitive to the L/G ratio and 2) the reboiler duty has a major effect on the regenerator performance. In Ref. [15] a model of the desorber is constructed according to model 3 where the aim is to try to minimize the energy consumption of the desorber. The main results show that by controlling the L/G ratio and reducing the steam flow rate by 10% it is possible to 1) increase the CO_2 removal by 1% and 2) to get a faster response of the desorber.

The models mentioned above are either of the absorber or the desorber and do not evaluate the behaviour of the whole capture plant. In Ref. [16] a dynamic model of the whole capture process is constructed according to model 3. The modelling environment used is gPROMS Advanced Model Library for Gas-Liquid contactors. The aim is to study the dynamic behaviour of the capture process when integrated with a power plant. The main results show that: 1) the ratio between the flue gas and the lean solvent entering the absorber is more important than the actual flow rates of those streams, 2) it is important to keep an appropriate water balance in the absorber, and 3) the response of the system is slow when the reboiler duty is changed.

In summary, a model of the whole absorption process which handles start-up, shut-down and other disturbances is still required in order to investigate the dynamic behaviour of the system. Furthermore, a simplified combined model of the capture process and the connected processes, that is, the flue gas train, the steam cycle and the CO_2 pipeline, is necessary to investigate how the processes will interact but has not yet been constructed.

3 Method

The method chapter includes a brief discussion about the modelling tool used in this thesis as well as important assumptions and limitations made in the thesis. Furthermore, the scenarios for load change are introduced, including the operating range investigated.

3.1 Modelling tool

In this thesis a dynamic modelling and simulation software called Dymola [33] is used for process simulations. Dymola is based on the Modelica [34] open standard language. This software is a suitable tool in this thesis because it can be used to simulate the dynamic behaviour of complex models including systems from many engineering domains, such as electrical, thermal, mechanical and chemical domains, unlike several other modelling tools which have been used for similar investigations. This makes it possible to connect the CO_2 capture model to models of a power plant and a CO_2 transfer pipe line.

3.2 Assumptions and limitations

The design and sizing of the CO_2 absorption system is not optimized as the technology, in combination with power plants, is under development and the knowledge about the geometry of full scale capture systems is limited. The model is not intended for column design computations, due to simplified assumptions regarding mass transport (discussed in detail in Chapter 4.1). The L/G ratio is calculated according to Equation 1:

$$L/G = \dot{n}_l/\dot{n}_g \tag{1}$$

where the $\dot{n}_l$ is the molar flow rate of the liquid solvent and the $\dot{n}_g$ is the molar flow rate of the flue gas entering the absorber. The L/G ratio is manipulated in order to reach capture efficiency of ~90% at 100% load. The model is not designed to simulate conditions of zero power output and flue gas mass flow, therefore, start-up and shut-down procedures are not simulated.

3.3 Effects of load changes

A coal fired power plant equipped with a post-combustion CO_2 capture system can vary the load depending on demand in two ways. It can either change the fuel input to the power plant or change the amount of steam delivered to the capture system. Thus two scenarios are investigated. In the first scenario the fuel input is reduced due to lowered energy demand. In the second scenario the steam delivered to the capture process is decreased due to peak demand and used instead for electricity production.

Scenario 1 - Part load operation

In this scenario the power plant operation is changed from full load down to 80%, 60% and 40% load by 5% per minute, which is a common rate of load change in coal fired power plants according to Ref. [17]. In the model, the flue gas mass flow rate decreases correspondingly to the load changes. The fuel composition and, therefore, flue gases composition is assumed to be constant. In this scenario no limits are set on the steam flow to the system which is controlled by keeping the lean loading of the solvent constant. The lean solvent loading is calculated according to Equation 2:

$$Lean\ solvent\ loading = \frac{\dot{n}_{CO_2}}{\dot{n}_{MEA}} \tag{2}$$

where $\dot{n}_{CO_2}$ is the molar flow of CO_2 leaving the desorber and $\dot{n}_{MEA}$ is the molar flow of MEA leaving the desorber. It is of interest to investigate and compare cases where no controls are added but also where controls are introduced to try maintaining a good system performance. In case 1 no controls are added whereas in cases 2 and 3 the capture efficiency and the L/G ratio respectively are controlled by varying the volume flow rate of the solvent into the absorber.

- **Case 1:** No additional control strategy applied (constant volume flow rate of solvent)
- **Case 2:** Capture efficiency controlled by varying the volume flow rate of solvent
- **Case 3:** L/G ratio controlled by varying the volume flow rate of solvent

It is of interest to study how load changes affect the capture process and how long it takes for the system to reach steady state. The output parameters studied are reboiler duty, rich solvent loading, the amount of steam supplied and amount of CO_2 delivered to the transportation network. It is also investigated how the capture efficiency and the L/G ratio change when they are not being controlled.

Scenario 2 – Peak demand

In this scenario the steam available for the reboiler is reduced with an open loop control by 10%, 30% and 50% negative step change as power plants might have to respond very quickly to increased demand [21]. The amount of flue gas entering the absorber is kept constant. Two cases are investigated, one where no control strategy is applied and another one where the lean loading is controlled by varying the volume flow rate of solvent to try maintaining a good system performance. In this scenario it is not of interest to control the efficiency and the L/G ratio like in the previous scenario because it is not possible to maintain the same efficiency when decreasing the energy input considerably. Also, the L/G ratio does not change during steam reduction because the amount of flue gas entering the absorber is constant.

- **Case 1:** No control strategy applied (constant volume flow rate of solvent)
- **Case 2:** Lean loading controlled by varying the volume flow rate of solvent

It is of interest to investigate how peak demand affect the amount of CO_2 delivered to the transportation network, the capture efficiency, the reboiler duty and the L/G ratio, and how long it will take for the system to reach steady state. In addition, the effects on the lean solvent loading are studied when it is not being controlled.

4 Model

The model used in the present work is based on the model presented by Åkesson et al. [**7**]. Chapter 4.1 gives an overview of the main features, including the main assumptions made. Chapter 4.2 discusses what discretization is needed in the columns to make the results grid independent. Chapter 4.3 and 4.4 describe the development made in this work of the reboiler model and the control strategies applied to the model, respectively.

4.1 Model review

The model describes the absorption of CO_2 from flue gas by 30 wt% MEA in water. Degradation of MEA is not considered and the MEA is assumed to be non-volatile, that is, no leakage of solvent, which means that injection of additional MEA is not required. The model is of type 3 in Figure 2-2, where a mass transfer rate between the liquid and the gas phase is considered and chemical reactions are assumed at equilibrium. Five main reactions between CO_2, MEA and water are considered in the system [7]:

$$2H_2O \leftrightarrow H_3O^+ + OH^-$$

$$CO_2 + 2H_2O \leftrightarrow H_3O^+ \; HCO_3^-$$

$$HCO_3^- + H_2O \leftrightarrow H_3O^+ + CO_3^{2-}$$

$$MEAH^+ + H_2O \leftrightarrow H_3O^+ + MEA$$

$$MEACOO^- + H_2O \leftrightarrow MEA + HCO_3^-$$

Both the absorber and desorber are modelled as packed columns. The columns are divided into several packed volumes and an ideally mixed sump volume in the bottom. The packing material serves the purpose of increasing the mass transfer area of the columns. The discretization of the packed volumes determines the accuracy of the results. All volumes include both liquid and gas bulk flows which are modelled as separate media with different properties. The ideal gas law is applied in the gas phase to compute the gas densities and pressure, and a constant density is used for the liquid. Pressure in both columns is determined by the gas phase pressure. The pressure drop in the columns is pre-defined. Insufficient wetting and flooding in column packings is not considered in the model.

Mass transfer between the gas and liquid phase is described by the two-film theory and thermodynamic equilibrium is assumed at the phase interphase. Mass transfer coefficients of water and CO_2 are determined according to Ref. [18] where an enhancement factor is used to describe the impact on mass transfer due to chemical reactions. Concentration and pressure gradients are used to compute the mass transfer between the bulk and the film for the liquid and gas phase, respectively. Mass and energy storage is only present in the bulk flows, but not in the film.

Chemical equilibrium is assumed at the phase interface and in bulk flows in all model parts. Reaction kinetics is therefore not taken into account. This is considered justified at high temperatures such as in the desorber. This assumption is also used in the absorber mainly because it simplifies the model and also due to lack of reliable kinetic data in literature. Hence, all chemical reactions are assumed to take place instantaneously which means that if the reaction rate between the solvent and CO_2 is slow, the model becomes inaccurate. This is, however, not the case for the reaction between MEA and CO_2 [19] and therefore this assumption is justified. Phase equilibrium at the interphase for both water and CO_2 is calculated by Henry´s law according to Ref. [20]. The speciation in the liquid phase is determined by equilibrium constants for each reaction given in Ref. [20].

The focus of the work is on the absorption process and the connected processes are treated as boundary conditions. The steam cycle, CO_2 pipeline, and flue gas train are described as a heat source, mass sink, and mass source respectively. Figure 4-1 presents the model as viewed in Dymola. All model components, represented with letters, are listed in Table 4-1 with a short description of their basic function. The components are divided into three categories: boundary conditions, process components and modelling/balancing components. The process components are included in the real system whereas the modelling/balancing components are necessary for the model to function properly. In addition all streams, represented with numbers, and their properties are listed in Table 4-2.

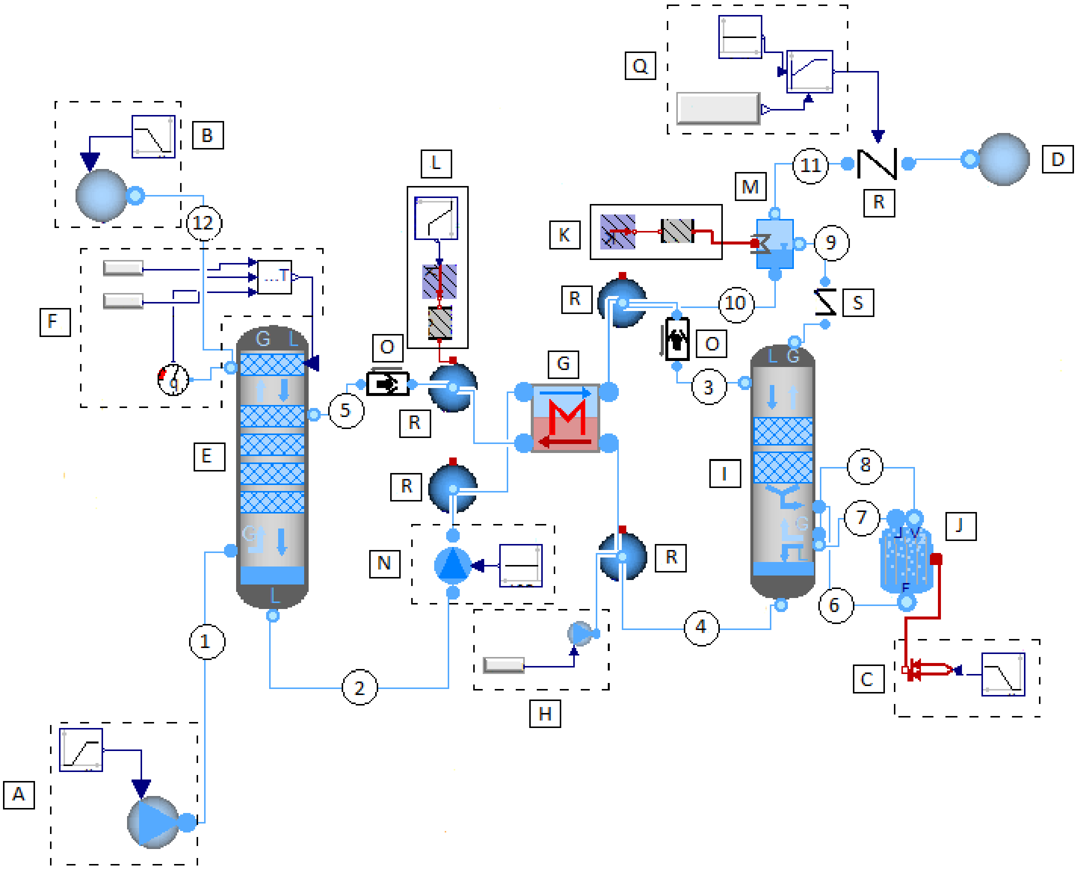

Figure 4-1: Flow diagram of the chemical absorption model in Dymola.

Table 4-1: List of components in the model. The letters represents the components in Figure 4-1.

	Boundary conditions	
A	Flue gas source	Supplies flue gas to the absorber with certain flow rate and flue gas composition
B	Flue gas sink	Receives cleaned flue gas from absorber
C	Heat source	Supplies heat to reboiler
D	CO_2 sink	Receives relatively pure CO_2 from the capture process
	Process components	
E	Absorber	Absorbs CO_2 from flue gas into the solvent
F	Temperature controller	Controls the fraction of steam in the flue gas leaving the absorber in order to minimize disturbances in the water balance of the system
G	Solvent heat exchanger	Exchanges heat between rich and lean solvent
H	Make up water flow control	Keeps the water content of the system constant
I	Desorber	Separates CO_2 from the solvent
J	Reboiler	Supplies heat to the desorber
K	Cooler	Removes heat to condenser/washer
L	Cooler	Cools down the lean solvent before entering the absorber
M	Condenser/washer	Reduces water content of CO_2 rich vapour from desorber
	Modelling/balancing components	
N	Solvent flow control	Controls volume flow rate of solvent in the system
O	Check valve	Ensures flow in one direction
P	Pressure controller	Controls pressure of CO_2 rich vapour entering CO_2 sink
Q	Control valve	Ensures a constant value of pressure of CO_2 rich vapour entering CO_2 sink
R	Volume	
S	Pressure valve	

Table 4-2: List of streams in the model. Composition, flow, temperature and pressure are listed for 100% load, 90% capture efficiency. The numbers represent the streams in Figure 4-1.

	1	**2**	**3**	**4**	**5**	**6**	**7**	**8**	**9**	**10**	**11**	**12**
Description	Flue gas entering the system	CO_2 rich solvent	CO_2 rich solvent	CO_2 lean solvent	CO_2 lean solvent	CO_2 rich solvent to reboiler	Liquid from reboiler	Vapour from reboiler	Vapour to washer	Water from washer	CO_2 rich gas to CO_2 sink	Cleaned flue gas
Composition												
CO_2	20.88	9.75	8.64	3.72	3.75	4.38	3.72	10.61	71.3	0	98.67	2.64
MEA	0	27.30	27.00	29.17	27.33	26.39	29.17	0	0	0	0	0
H_2O	7.54	62.93	64.36	67.11	68.92	69.23	67.11	89.39	28.7	100	1.33	9.49
O_2	3.42	0	0	0	0	0	0	0	0	0	0	4.19
N_2	68.16	0	0	0	0	0	0	0	0	0	0	83.68
Flow [kg/s]	1.5	4.84	4.59	4.2	4.21	4.64	4.2	0.44	0.39	0.11	0.28	1.22
Temp. [°C]	50	58	110	120	40	119	120	120	102	35	35	53
Pressure [bar]	1.03	1.46	1.85	2.93	1.00	1.86	1.86	1.86	1.85	1.87	1.80	1.00

Data on flue gas composition from Nordjyllandsværket (NJV) is used as an input parameter in model simulations. NJV is a modern 411 MW_{el} coal-fired power plant, located in Denmark. The flue gas is saturated with water at 50°C and 1 bar before entering the absorber. The flue gas composition after the boiler and at the absorber inlet is given in Table 4-3.

Table 4-3: Flue gas composition after the boiler and at the absorber inlet.

	After boiler	**Inlet of absorber**
Compound	**Mass %**	**Mass %**
CO_2	21.37	20.88
N_2	70.15	68.17
H_2O	5.41	7.54
O_2	3.07	3.42

4.2 Discretization

In this chapter, the required level of discretization in both columns is studied. Different L/G ratios in the system may require different discretization of the packed segments in order to calculate the concentration gradients and temperature profiles independent of discretization. The number of packed segments in the absorber and the desorber are 4 and 2, respectively. A discretization in the columns is chosen such that it does not affect the results in the entire investigated range of L/G ratios.

The absorber column is studied separately to avoid disturbing effects from other model parts. The L/G ratio can be manipulated directly in the stand-alone absorber by changing the flue gas and solvent flow rate via boundary conditions. Variations in capture efficiency are studied and used to determine the required level of discretization in the absorber.

The effects on the desorber are not studied in the same way as for the absorber. The main reason for this is that the L/G ratio cannot be varied directly through boundary conditions in the stand-alone desorber. The boundary conditions would have to be determined from running the whole model which makes it not interesting to study the desorber alone. Instead the effect of changing the discretization in the desorber on the reboiler duty (MJ/kg CO_2 captured) and capture efficiency in the whole model is studied. This is done only in the tuned model, with 90% efficiency.

Figure 4-2 shows how the discretization of the packed segments in the absorber affects the capture efficiency with different L/G ratios. Dividing each packed segments into 7 volumes, 28 volumes in the whole column, results in a difference of less than 0.1% points in capture efficiency compared to simulations with 10 volumes in each segment. Increased discretization also results in longer simulation time and it is therefore decided to use 7 volumes in each packed segment in the absorber.

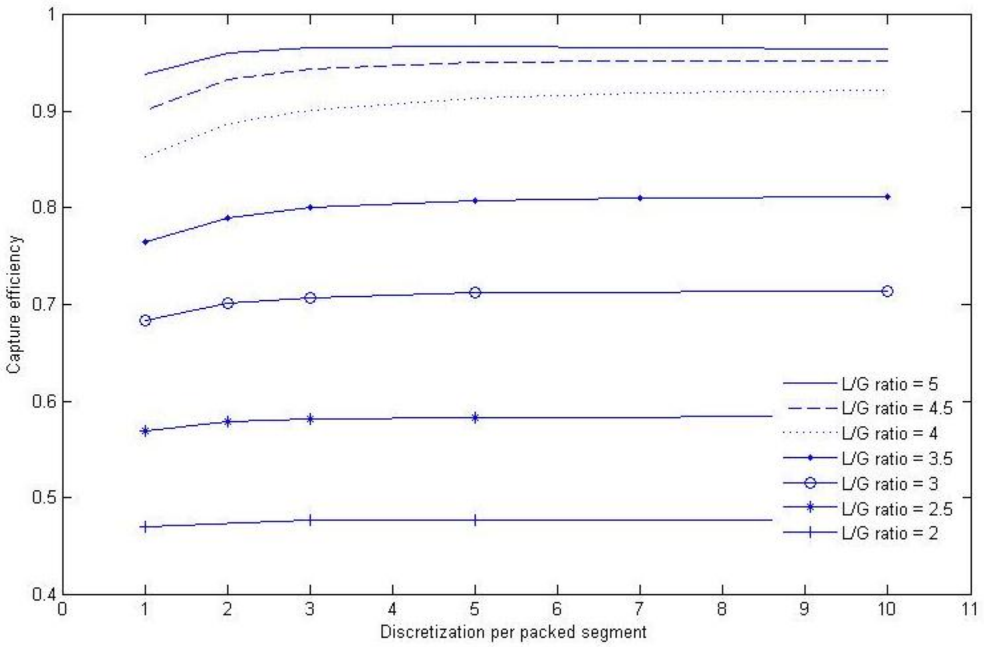

Figure 4-2: Impact of different discretization per packed segment in the absorber on capture efficiency with different L/G ratios.

Figure 4-3 shows how the discretization of the packed segments in the desorber affects the capture efficiency and the reboiler duty. Dividing each packed segment into 7 volumes is sufficient to produce grid independent results in the desorber.

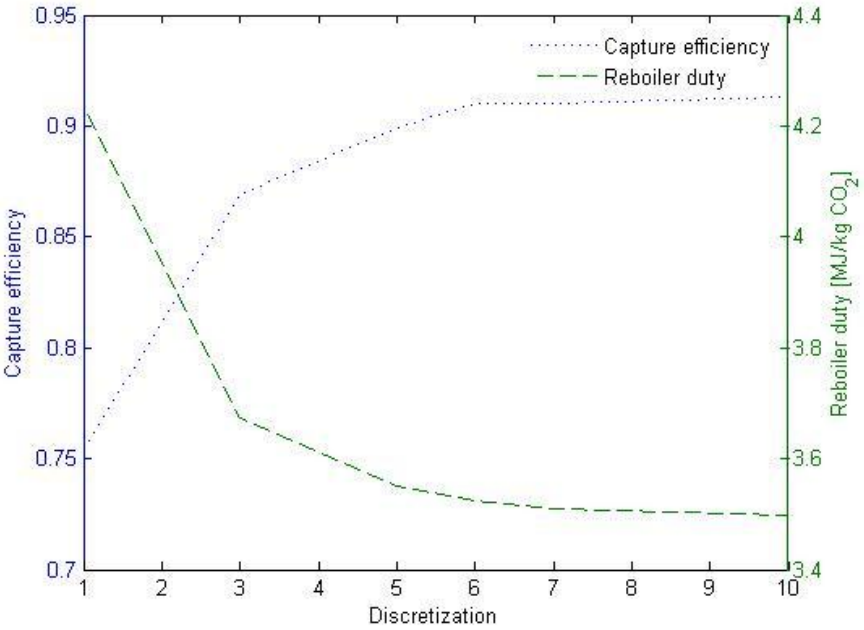

Figure 4-3: Impact of discretization per packed segment in the desorber on capture efficiency and reboiler duty.

4.3 Development of reboiler model

The reboiler is modelled as a once-through shell-and-tube type heat exchanger and is based on an existing model from the Modelica Library CombiPlantLib, where MEA-CO_2-H_2O solution is in the tubes and steam is in the shell. The reboiler model is divided into two parts: steam side and a solution side. The reboiler is constructed in such way that the geometrical and initialization parameters of both steam and solution side are accessible and adjustable at the top level of the model. The steam side consists of a steam inlet, condensate outlet, two heat transfer models and a tube wall. The solution side is based on Ref. [7] and consists of a liquid inlet, two outlets, one gas and one liquid, and a heat port. Before the reboiler development, a heat source boundary condition, in which a heat rate to the solution side is set, is connected to the heat port. The solution side is modelled as a single flash volume, that is, the solution side has the same properties in the entire volume and thus, no temperature gradient exists in the volume. In addition, no heat transfer resistance is modelled on the solution side. This means that all the heat supplied via the heat port is delivered to the fluid in the solution side. The steam side is connected to the solution side via heat port on the tube wall which transfers heat from both heat transfer models. A graphical representation of the model construction can be seen in Figure 4-4.

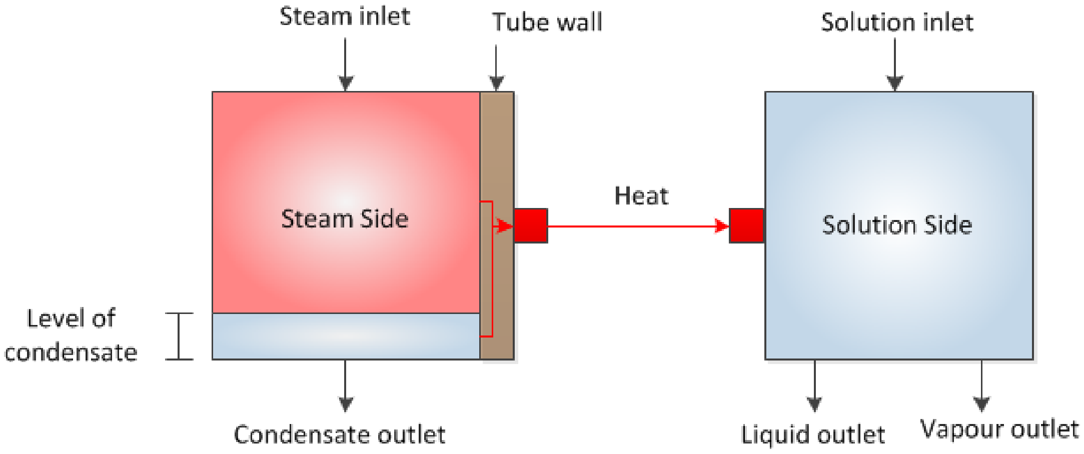

Figure 4-4: A graphical representation of the reboiler model construction.

The amount of heat transferred from each heat transfer model depends on the condensate level within the reboiler shell which is calculated in the model. The two heat transfer models calculate the heat transferred from the condensing steam and the liquid condensate separately because the heat transfer coefficient is much lower for the condensate than for the condensing steam. This makes it possible to control the reboiler duty either by controlling the amount of steam entering the reboiler or by controlling the condensate level. The heat transferred by condensation over the tubes and by convection from the condensate is calculated according to Equation 3 [23]:

$$\dot{Q} = \alpha * A * (T - T_s) \tag{3}$$

where α is the heat transfer coefficient, A is the heat transfer area, T is the temperature of the steam or the condensate and T_s is the temperature of the MEA-CO_2-H_2O solution in the tubes. The relative level of condensate within the reboiler is calculated in the model and is used to calculate the heat transfer area in Equation 3 for both the condensing steam and the condensate according to Equations 4 and 5:

$$A_{steam} = A_{tot} * (1 - y) \tag{4}$$

$$A_{liq} = A_{tot} * y \tag{5}$$

where A_{steam} is the heat transfer area of the condensing steam, A_{tot} is the total heat transfer area of the tubes, y is the relative level of condensate and A_{liq} is the heat transfer area of the liquid condensate.

The condensate flowing out from the bottom of the shell is treated as a single-phase pipe flow of a Newtonian fluid. The flow is assumed thermally and hydraulically developed and constant wall temperature is assumed. The heat transfer coefficient for both the condensing steam and the condensate flowing out of the reboiler is calculated according to Equation 6 [23]:

$$\alpha = \frac{Nu * \lambda}{d_{hyd}} \tag{6}$$

where Nu is the Nusselt number, λ is the conductivity of the fluid and d_{hyd} is the hydraulic diameter of the pipe. The mean Nusselt number for heat transfer by convection from the liquid condensate is calculated according to correlations from Ref. [24]. The reboiler has horizontal orientation and therefore correlation for film condensation over horizontal tube bundles is used according to Ref. [22] when calculating the Nusselt number for the condensing steam.

Before the reboiler development, the component only consisted of the solution side, described above and a heat port which made a connection to a steam cycle model not possible. The developed reboiler model makes this connection possible. Separate heat transfer models for the steam and the condensate are applied which makes it possible to control the heat demand of the reboiler by either controlling the amount of steam entering the reboiler or the amount of condensate exiting, as is explained in Chapter 4-4. Figure 4-5 illustrates the major differences before and after the development.

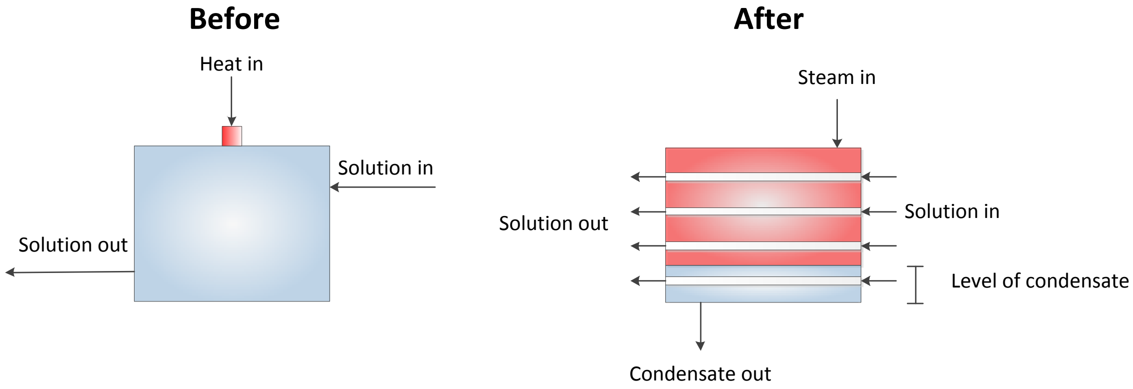

Figure 4-5: Comparison of reboiler components before and after development.

The new reboiler component is tested in order to create results that show the effects of the condensate level on the heat transferred. The results from this test are presented in Table 4-4 and show that the condensate level within the reboiler has an effect on the heat transferred from the steam side to the solution side of the reboiler. With higher condensate level, the heat transferred from the condensing steam decreases while the heat is transferred from the condensate flowing out of the reboiler increases. The results also show that considerably less heat is transferred from the condensate than the condensing steam, as expected.

Table 4-4: Results from reboiler component test.

Relative level height	Heat transferred from condensing steam [kW]	Heat transferred from condensate [kW]	Total [kW]
0.01	1642	4	1646
0.85	1011	211	1222

4.4 Development of control strategies

When investigating the effect of load changes, it is of great interest to see how the energy demand of the process and the system performance changes. This requires a control system with closed loop control, which is not included in the model by Åkesson et al [7]. The Åkesson model includes open loop control for the heat supplied to the reboiler and the solvent flow rate. This means that these two parameters can be varied but not related to changes in operating conditions, such as the ones investigated in this thesis. In this work, four closed loop controls are developed for the two scenarios studied which are discussed in Chapters 4.4.1 and 4.4.2. A summary of the control strategies used for both scenarios is presented in Table 4-5.

Table 4-5: Summary of control strategies for both scenarios.

Scenario	Controlled variable	Manipulated variable	Set point
1	Lean solvent loading	Steam flow to reboiler	0.18 [mol CO_2/mol MEA]
1	Capture efficiency	Solvent flow rate	90 %
1	L/G ratio	Solvent flow rate	3.55 [mol·s^{-1} liq/ mol·s^{-1} gas]
2	Lean solvent loading	Solvent flow rate	0.18 [mol CO_2/mol MEA]

The controller which is used for the closed loop controls described below is a typical PID (Proportional–Integral–Derivative) controller. The controller receives two input signals, a measured value and a set value. The controller compares these signals and minimizes the discrepancy. Figure 4-4, illustrates the function of the PID controller. In the cases where the PID controller is used in combination with control valves, a limiter is added, which ensures that the output signal is between zero and one, zero meaning that the valve is fully closed and one meaning that it is fully open. Tuning of the PID controllers is performed by the empirical Ziegler-Nichols method [25].

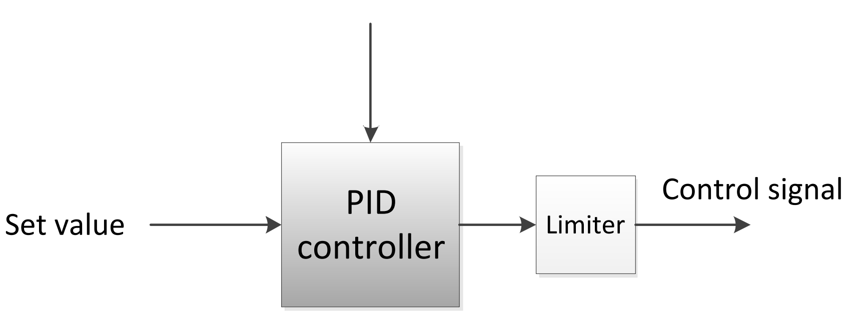

Figure 4-6: PID controller with limited output in Dymola.

4.4.1 Control strategies for scenario 1 – Part load operation

The lean solvent loading is controlled by manipulating the heat supplied to the process in scenario 1. It is important to control the lean solvent loading because if it is too high, the performance of the absorber becomes poor and therefore the capture efficiency decreases. On the other hand, if the lean solvent loading is too low, more energy is required in the desorber for separating CO_2 from the solvent.

Load changes have a direct effect on the heat supplied to the reboiler and thus the lean solvent loading. Two strategies are investigated to control the amount of heat transferred from the steam side to the solution side in the reboiler in order to achieve a desired lean solvent loading, see Figure 4-7. The first one involves controlling the flow of the incoming steam through a control valve. By controlling the flow it is possible to control the temperature and the pressure of the inflowing steam and thus the amount of heat transferred to the solution side. For this control scheme, an additional controller is applied on the outflowing condensate to ensure a constant condensate level within the reboiler. This prevents the reboiler from filling up with condensate or becoming completely drained. Too high condensate level results in poor reboiler performance and can also damage the reboiler for example by corrosion [26]. On the other hand, if all the condensate is drained from the shell, steam will flow out of the reboiler which is uneconomical and could have damaging effects on the condensate pipeline system [26].

The second control strategy involves controlling the condensate level within the reboiler shell by using a control valve that controls the flow of condensate out of the reboiler. By doing so, the heat transferred from the steam side to the solution side is controlled by changing the condensate level and thereby the heat transfer area of the steam. Higher condensate level decreases the heat transfer area of the steam and therefore decreases the total heat transferred to the solution side. Dynamic responses of both strategies are studied in Chapter 5.4 and it is determined which strategy is more suitable when investigating effects of part load operation.

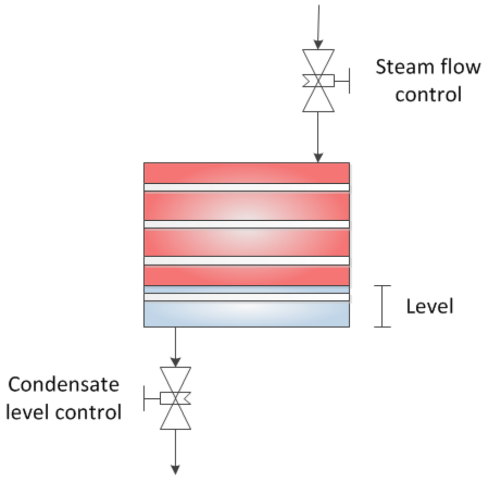

Figure 4-7: Two strategies to control the amount of heat transferred in the reboiler.

It is also of interest to construct a control system which controls either the capture efficiency or the L/G ratio when investigating the effect of part load operation on the capture process. Both the L/G ratio and the efficiency are controlled by manipulating the solvent volume flow rate. Figure 4-8 shows how control strategies for the lean solvent loading, capture efficiency or the L/G ratio are implemented in the capture process.

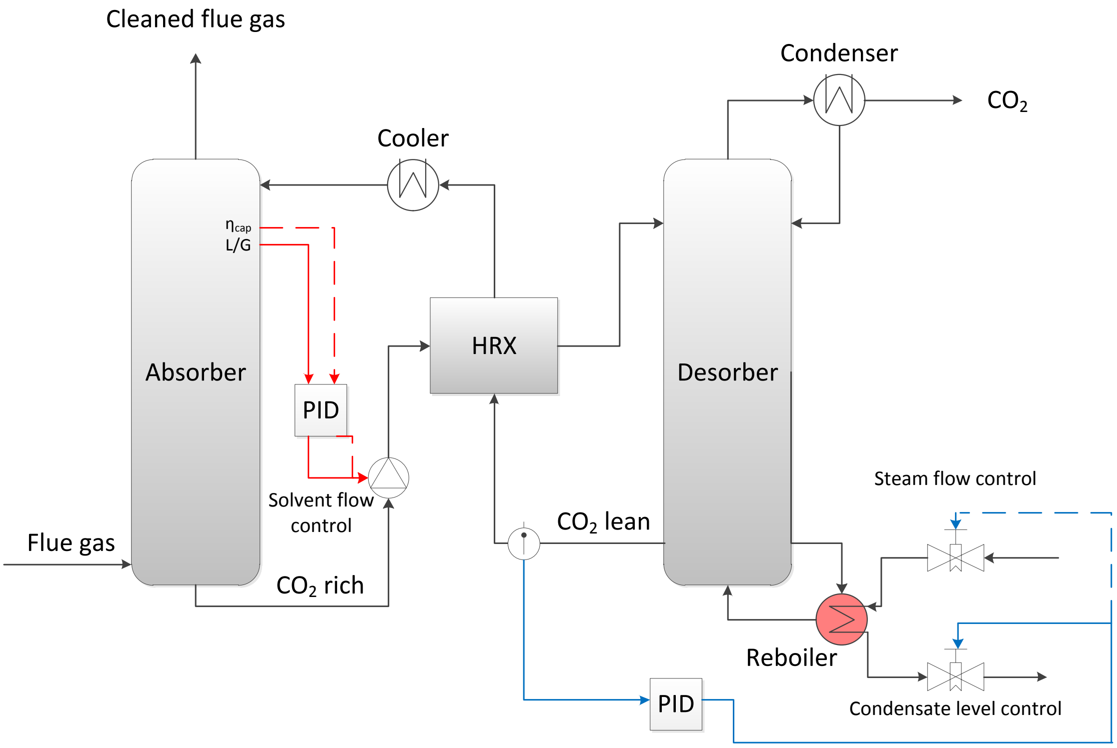
Cleaned flue gas
Condenser
CO2
Cooler
ηcap
L/G
HRX
Absorber
Desorber
PID
Solvent flow control
Steam flow control
CO2 lean
Flue gas
CO2 rich
Reboiler
PID
Condensate level control

Figure 4-8: Implementation of control strategies in scenario 1 for lean loading, capture efficiency and L/G ratio in the capture process.

4.4.2 Control strategies for scenario 2 – Limited steam availability

In scenario 2, the lean solvent loading is controlled by manipulating the volume flow rate of the solvent instead of manipulating the heat supplied to the process as done in scenario 1. By varying the solvent flow rate it is possible to keep the lean loading constant during periods of limited steam availability and thus avoid recirculating larger flows of solvent in the system than needed. Figure 4-9 shows how the control strategy for lean solvent loading is implemented in the capture process.

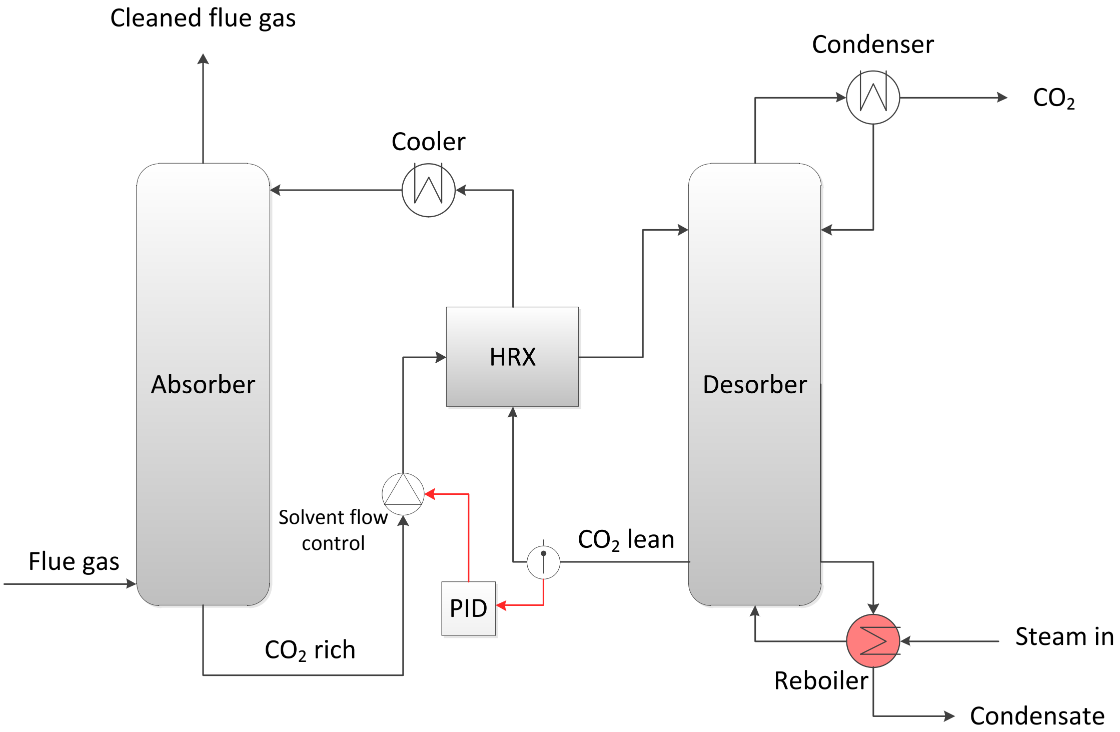
Cleaned flue gas
Condenser
CO_2
Cooler
Absorber
HRX
Desorber
Solvent flow control
CO_2 lean
Flue gas
PID
Steam in
CO_2 rich
Reboiler
Condensate

Figure 4-9: Implementation of a control strategy in scenario 2 for lean solvent loading in the capture process.

5 Results – Model development

This chapter includes results from a parametric study performed where the system is tuned to reach 90% capture efficiency and the effect of geometrical design parameters on the system behaviour is studied. It also includes results which show how different L/G ratios affect the capture efficiency. Finally, results from comparing control strategies for the reboiler model are presented and a suitable strategy is selected.

5.1 Parametric study - Tuning of system

The system is tuned to reach 90% efficiency at full load by setting the flue gas mass flow rate to 1.5 kg/s and the solvent volume flow rate to 16 m^3/hour, which results in a L/G ratio of 3.55. In order to get a better understanding of the system behaviour, the operating and equilibrium lines between the top and the bottom of the absorber are plotted in Figure 5-1. Those lines describe the mole fraction of CO_2 in the gas versus mole fraction of CO_2 in the liquid for operating and equilibrium conditions in the column. The equilibrium conditions are calculated from the liquid temperature which varies throughout the column. The driving force for the mass transfer is represented by the gap between the two lines, that is, the closer the operating line is to the equilibrium line, less mass is transferred between the liquid phase and the gas phase. A near-equilibrium operation at the top or the bottom of the column indicates an excess or insufficient flow of solvent relative to the incoming CO_2 in the system, respectively [28]. As can be seen in Figure 5-1 on the left-hand side, the operating line does not reach the equilibrium line anywhere along the column, which indicates a good column performance at 90% capture efficiency. It can also be seen that the driving force for mass transfer seems to be larger at the top of the column than at the bottom.

On the right-hand side in Figure 5-1, the liquid and gas temperature profiles in the absorber are plotted. The liquid and gas temperature profiles are similar in size and shape, but the slight difference is due to a difference in heat capacities of the two phases [28]. In the upper part of the absorber the temperature rises before it decreases again in the top. This temperature profile is often referred to as the temperature bulge, which is due to combined effects of water condensation and vaporization and absorption in the column [28]. According to Kvamsdal and Rochelle [28], the temperature bulge tends to occur in the column where the largest absorption rate can be found. In this case, the bulge is located near the top of the column which indicates that the greatest absorption rate is also near the top. This complies with the smaller distance between the operating and equilibrium line at this position seen in the left figure.

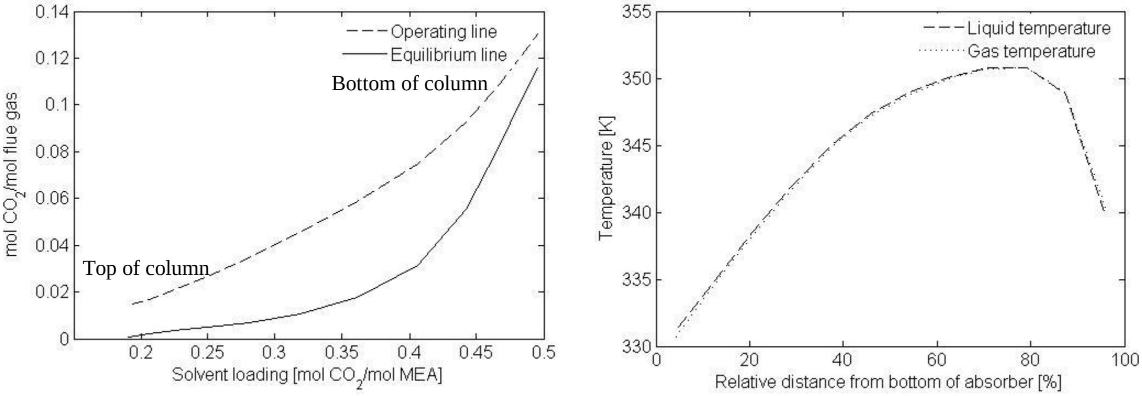

Figure 5-1: Equilibrium and operating lines for the absorber (left) and liquid and gas temperature profiles (right) for the tuned system.

5.2 Parametric study - Effect of geometrical design parameters

The diameter of the absorption column is varied from 0.25 m to 3 m in order to study its impact on the capture efficiency. The impact of diameter variations on the capture efficiency and residence time is shown in Figure 5-2. The residence time of the liquid and gas phases, which is often used in column design to determine the necessary column height [29], is approximated according to Equation 7:

$$t_{res} = V_{fluid}/\dot{V}_{fluid} \tag{7}$$

where t_{res} is the residence time, V_{fluid} is the volume of either the gas or the liquid and $\dot{V}_{fluid}$ is the volume flow rate of the fluid. Geometrical variations of the column result in the same proportional change of the liquid and gas residence time. Therefore only the liquid residence time is plotted in the figure below. The diameter of the absorber in the model is 0.5 m and is marked with a circle in the figure. Other input parameters are kept constant but variations in column diameter also affect variables, such as mass transfer area and the fluid velocities. The superficial gas velocity is the gas velocity if no packing material or solvent is present in the column and is approximated according to Equation 8:

$$v_s = \dot{V}_g/A_{cross} \tag{8}$$

where v_s is the superficial gas velocity, $\dot{V}_g$ is the gas volume flow rate and A_{cross} is the cross sectional area of the absorber. The superficial gas velocity is closely connected to the diameter and is often used in column design to determine the optimal column diameter [29]. It can be seen that increasing the diameter above 1 meter has little effect on the efficiency, however when the diameter is decreased, the capture efficiency decreases considerably. Figure 5-3 shows the equilibrium and operating lines for the absorber when the diameter has been increased to 3 m on the left hand side and decreased to 0.25 m on the right hand side. When the diameter is increased the column is operating close to equilibrium and near the bottom the operating line reaches the equilibrium line. This indicates that there is insufficient flow of solvent relative to the incoming CO_2 in the system as expected from Figure 5-1. When the diameter is decreased, the mass transfer area and the residence time decrease which has a negative

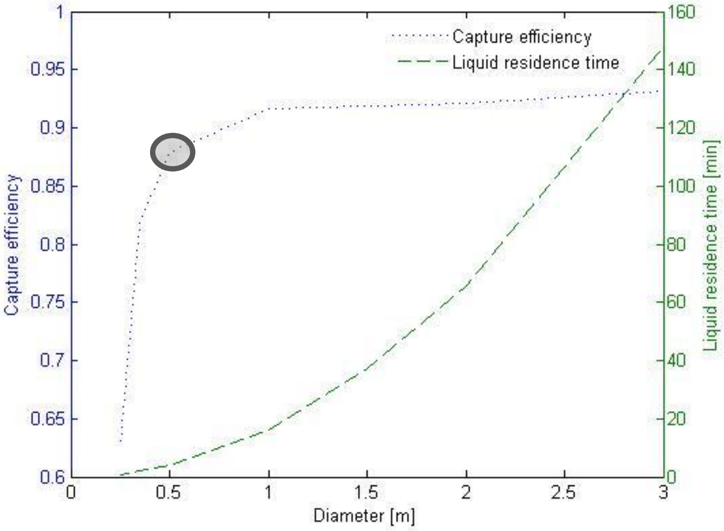

Figure 5-2: Effect of diameter variations on capture efficiency and residence time.

impact on the capture efficiency, as seen in Figure 5-2. The negative effect of decreasing the diameter becomes clear when Figure 5-3 is studied. The absorber is not reaching equilibrium anywhere along the column which indicates that there is enough solvent flow to handle the incoming CO_2. The system is therefore limited by other factors, such as mass transfer area, residence time and the gas velocity as the pressure drop increases and mixing between the phases decreases [29]. Varying the height of the absorber has the same effect on the capture efficiency as varying the absorber diameter. The packing height of each section is varied in proportion to the total height. The height of the absorber in the model is 25 m.

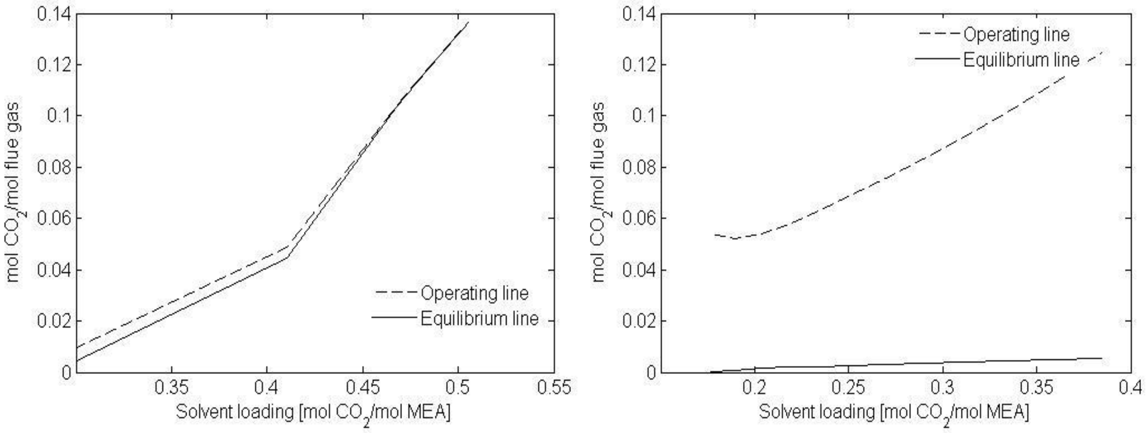

Figure 5-3: Equilibrium and operating lines for the absorber when the diameter has been increased to 3 m (left) and decreased to 0.25 m (right).

Varying the geometrical design parameters in the desorber has little effect on the capture efficiency (not shown in figures). The design parameters are; diameter 0.5 m and height 20 m. A decrease in the diameter down to 0.25 m decreases the capture efficiency around 1.5%. Decreasing the height down to 14 m decreases the capture efficiency around 2.5%. An increase in the diameter or the height up to 1 m and 24 m, respectively, has almost no effect on the efficiency or an increase of less than 0.3%. These results show that at current operating conditions the size of the desorber could be decreased without a major effect on the system performance. Changing the operating conditions, such as increasing the temperature and pressure could, however, give different result but in a real system that would cause degradation of the solvent [32]. Different operating conditions in the desorber are therefore not investigated.

In summary, the geometry of the absorber has a greater effect on the capture efficiency than the geometry of the desorber at the current operating conditions. It is important that the absorber is large enough to handle the flue gas flows, otherwise it starts to affect the mass transfer area, gas velocity and residence time which results in lower capture efficiency.

5.3 Impact of L/G ratio on capture efficiency

Figure 5-4 shows how different L/G ratios affect the capture efficiency in the absorber and it can be seen that lower L/G ratio results in lower capture efficiency.

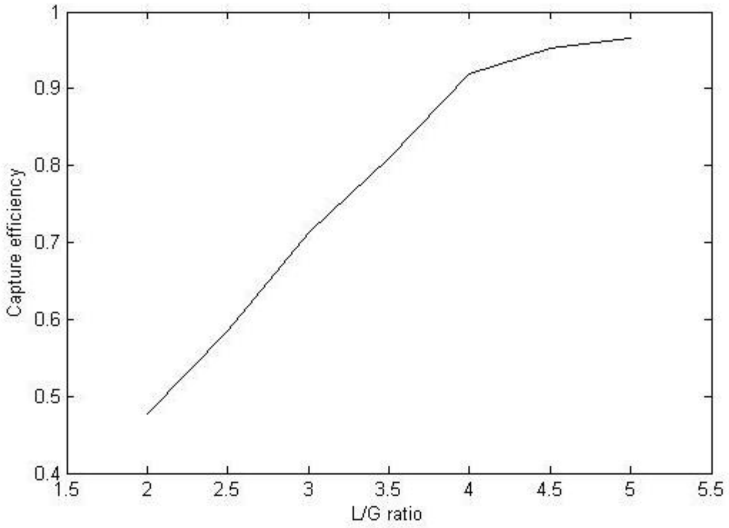

Figure 5-4: Effect of different L/G ratio on capture efficiency in the absorber.

To get a better understanding of this trend the operating and equilibrium lines for the absorber with L/G ratios of 5 and 2 are plotted in Figure 5-5. On the left hand side, it can be seen that the operating and equilibrium lines for a L/G ratio of 2 in the absorber are very close to each other at the bottom of the column. This indicates that there is insufficient solvent flow in the system, thus the L/G ratio is too low and limits the capture efficiency. For the system with a L/G ratio of 5, on the right hand side, the opposite is observed. The operation line is close to the equilibrium line at the top of the column and thus the greatest absorption rate is found at the bottom. This also means that there is excess solvent in the system as expected.

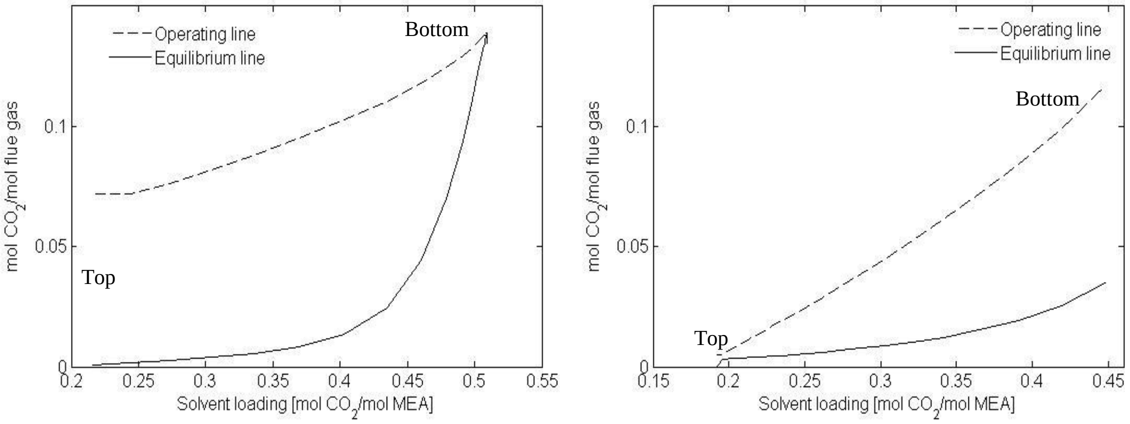

Figure 5-5: Operating and equilibrium lines for absorber with L/G ratio = 2 (left) and with L/G ratio = 5 (right).

The liquid and gas temperature profiles of the absorber are observed in Figure 5-6 for L/G ratio of 2 and 5. On the left hand side, it can be seen that the temperature bulge is located at the top of the column, when the L/G ratio is 2, which indicates that the greatest absorption rate is found at the top of the column. This complies with the findings of Kvamsdal and Rochelle [28] where it is also pointed out that a temperature bulge near the top of an absorber column indicates that the L/G ratio of the column is relatively low. On the right hand side, when the L/G ratio is 5, the highest temperatures are found in the bottom of the absorber. The temperature bulge for this system is not as definitive as the one for the system with relatively low L/G ratio but it still points to that the system has relatively high L/G ratio.

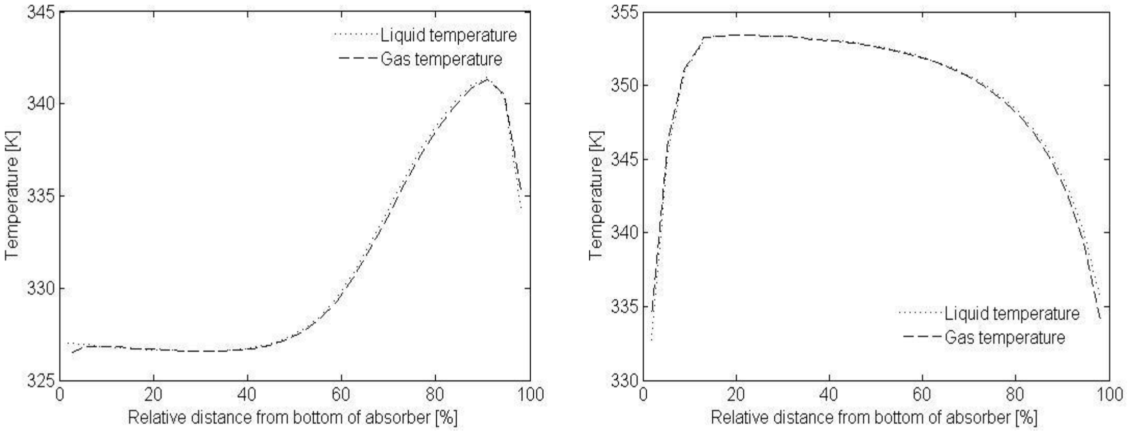

Figure 5-6: Liquid and gas temperature profiles for absorber with L/G ratio = 2 (left) and with L/G ratio =5 (right).

In this study, different flow rates of flue gas and solvent which produce the same L/G ratio are investigated in the stand-alone absorber. The resulting capture efficiency is roughly the same for the different flows. This indicates that the L/G ratio is more important than the actual flow rates for maintaining a desired capture efficiency which is in accordance with Ref. [28]. However, this only applies when the size of the system, and thus the mass transfer area and the residence time are not limiting the process.

5.4 Selection of reboiler control strategy

Two strategies for controlling the lean solvent loading in scenario 1 are investigated. The dynamic response determines which of those strategies should be used when investigating the effects of part load operation. All boundary conditions in the tuned system are kept constant during the simulations. Figure 5-7 shows the dynamic responses of the steam flow and the condensate level control strategies. It can be seen from the left figure that when the steam flow control strategy is used it is possible to reach the desired lean loading with less than 1% deviation from the set value in around 8 simulation minutes. For the condensate level control strategy, the desired lean loading, with less than 1% deviation from the set value, is not reached until the model has been simulated around 415 minutes, or around 7 hours. The dynamic response is faster for the steam flow control strategy and the overshoot is also considerably smaller. In the steam flow control strategy, manipulating the steam inlet valve immediately affects the amount of steam entering the reboiler. Consequently the shell temperature and pressure and the amount of heat that can be transferred are affected. On the other hand, changing the position of the condensate valve does not have a direct effect on the steam flow, instead it affects the level of condensate which in turn affects the heat transfer area which finally affects the amount of heat transferred, resulting in a slower dynamic response. The steam flow control strategy is therefore favoured over the condensate level control when investigating the effects of part load operation.

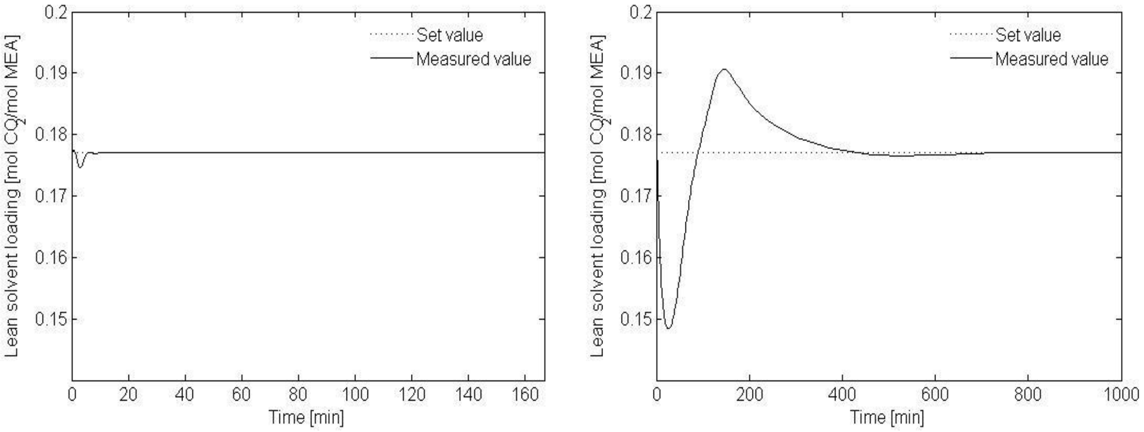

Figure 5-7: Dynamic response of the steam flow control strategy (left) and the condensate level control strategy (right). Please note the different scales on the x-axis.

6 Results – Effects of load changes

This chapter includes results and discussions on the transient behaviour of the MEA absorption process during load and steam reduction scenarios, introduced in Chapter 3.3.

6.1 Scenario 1 – Part load operation

Figure 6-1 shows the results from cases 1, 2 and 3 when the load is reduced from 100% down to 80%. The load reduction takes 4 minutes and starts after the process has been simulated for 5000 seconds (around 83 minutes) to ensure that the process has reached steady state before the load is reduced. The lean loading is kept constant in all cases.

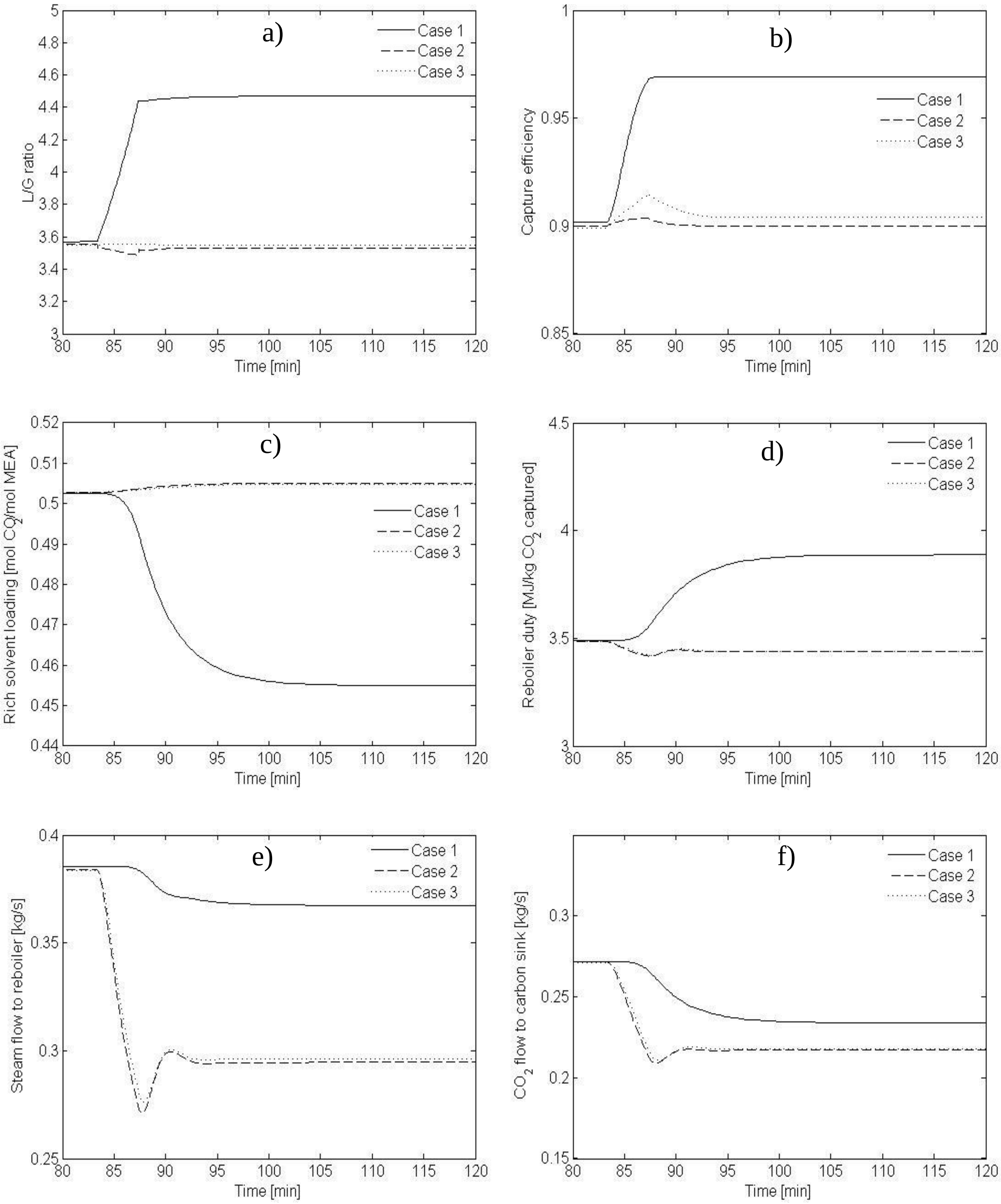

Figure 6-1: Effect of load reduction from 100% to 80% load for case 1, 2 and 3.

Figure a) shows how the L/G ratio increases in case 1 by ~25% whereas in cases 2 and 3 there are little changes. The large increase in case 1 can be explained by the constant liquid flow into the absorber while the flue gas flow is reduced. The increase in L/G ratio in case 1 increases the capture efficiency up to ~97% as can be seen in Figure b). In case 2 it takes few minutes for the controller to bring the efficiency down to 90% and in case 3 the load reduction causes a slight increase in capture efficiency. The transient behaviour of the rich loading can be observed in Figure c). Cases 2 and 3 show the same behaviour where the rich loading increases slightly. However in case 1 the rich loading decreases by ~9% because of excess solvent in the system.

Before the load is reduced the reboiler duty is ~3.5 MJ/kg CO_2 captured, see Figure d). Cases 2 and 3 show the same behaviour, a slight decrease with a minor bump. In case 1 the decrease in rich solvent loading causes the reboiler duty to increase by ~11% because of higher driving forces for solvent regeneration in the desorber. In all the cases the steam flow to the reboiler decreases because of less flue gas entering the system, resulting in less steam needed for regeneration in the desorber, see Figure e). However, the amount of steam reduced is less in case 1 than in cases 2 and 3 due to the higher reboiler duty. The overshoot seen in Figure e) is due to control action. The CO_2 flow out of the desorber is higher in case 1 than in cases 2 and 3 due to higher capture efficiency, see Figure f).

It can be seen from the results that it takes longer time for the system to reach steady state in case 1 than in the other two cases or around 30 minutes and 20 minutes respectively. Furthermore, it generally takes longer time for the system to reach steady state the further the load is reduced. The overall results of load reduction down to 80%, 60% and 40% load are presented in Table 6-1. The same figures for the 60% and 40% load cases as for the 80% case can be observed in Appendix A. Similar results are seen for the larger load reductions, however larger variations are observed with larger load reductions as can be seen in the table. It also takes longer time for the controllers to reach the set value in cases 2 and 3.

It can be seen from Table 6-1 that the system response to the load reduction is around 20 seconds, although it takes longer for some of the variables to start responding to the load changes. The load reduction has a direct effect on the L/G ratio and the capture efficiency which results in quicker response of these variables than the others. The response time in case 1 is longer than in cases 2 and 3 for most of the variables, as can be seen from Table 6-1, but is in all cases 2 minutes or less. The rise time, which is the time it takes for the variable to reach 90% of the difference between the two steady state values before and after load reduction, is presented in the table. The rise time is higher in case 1 than in cases 2 and 3 for all the variables except the rich solvent loading, and increases with increased load reduction. The changes observed in the rich solvent loading are however relatively small compared to the other variables, as seen in the table.

Table 6-1: Main results from all load reductions.

Variable	**Case**	**Response time (seconds)**	**Rise time (minutes)**			**Change (%)**		
Load change			**80 %**	**60 %**	**40 %**	**80 %**	**60 %**	**40 %**
L/G ratio	1	20	4	7.5	15	+ 25	+ 69	+ 157
	2	20	0	1	2	- 1.5	- 1	- 1
	3	-	-	-	-	-	-	-
Capture efficiency	1	20	3	5	10	+ 8	+ 9	+ 11
	2	-	-	-	-	-	-	-
	3	20	1	2	2	+ 0.5	+ 1	+ 1
Rich solvent loading	1	35	11	13	15	- 9	- 23	- 36
	2	30	11	17	24	+ 0.5	+ 0.5	+ 1
	3	30	11	17	24	+ 0.5	+ 0.5	+ 1
Reboiler duty	1	50	12	15	18	+ 11%	+ 39	+ 91
	2	20	5	6	9	- 1.5	- 2.5	- 4
	3	20	5	6	9	- 1.5	- 2.5	- 4
Steam flow to reboiler	1	90	13	13	19	- 4.5	- 10	- 18
	2	20	3	6	10	- 23	- 45	- 66
	3	20	3	6	10	- 23	- 45	- 66
CO_2 flow to carbon sink	1	60	12	14	16	-14	- 35	- 56
	2	20	4	7	11	- 23	- 40	- 60
	3	20	4	7	11	- 23	- 40	- 60

6.1.1 Discussion

The results presented above comply with the findings of Kvamsdal et al. [13] and Lawal et al. [16], where effects of load reduction on a stand-alone absorber and the whole capture process are investigated, respectively. When changing from full load operation to part load the capture efficiency will increase if the solvent volume flow rate is kept constant because the L/G ratio increases. This also means that the rich loading of the solvent decreases and the flow rate of the solvent is higher than needed which results in a certain waste of energy in the system.

It is evident from the results presented above that in order to minimize the energy penalty of the capture process, during transition and at the new steady state, a control strategy is required. However, it is not completely evident which parameters should be controlled. Cases 2 and 3 give similar results, so controlling either the efficiency or the L/G ratio results in less energy needed to operate the process after the load has been reduced. It is worth mentioning that when the capture efficiency is kept constant it is possible to decrease the solvent flow rate more than the corresponding decrease in flue gas flow due to the increased rich loading. The load reduction causes little fluctuations and the curves are generally rather smooth, with little overshoots. The overshoots could be minimized by further tuning of the controllers and a slower load change would make the curves even smoother.

By doing simple calculations based on the results presented above it is possible to estimate roughly how much heat is needed for the reboiler in the absorption process if applied to NJV and how much energy is saved by using the control strategies proposed. The mass flow of flue gas from NJV is around 370 kg/s when the power plant is running at 100% load. The heat needed for the process is estimated at steady state before load reduction and at steady state after the load has been reduced. This is done according to Equation 9:

$$\dot{Q}_{process} = q_{reboiler} * \dot{m}_{CO_2} \tag{9}$$

where $\dot{Q}_{process}$ is the heat demand of the capture process, $q_{reboiler}$ is the reboiler duty and $\dot{m}_{CO_2}$ is the mass flow rate of CO_2 captured from NJV depending on load. Results from these calculations are presented in Table 6-2. It can be seen from the results that applying capture efficiency control as done in case 2 results in the lowest reboiler energy demand. Implementation of L/G ratio control in case 3 results in similar energy demand, however slightly higher than in case 2.

Table 6-2: Roughly estimated heat demand of the capture process in Scenario 1 when applied to NJV.

Load	**100%**		**80 %**		**60 %**		**40 %**	
	MW	MJ/kg CO_2	MW	MJ/kg CO_2	MW	MJ/kg CO_2	MW	MJ/kg CO_2
Case 1	233.0	3.487	224.3	3.887	211.8	4.836	196.1	6.631
Case 2	233.0	3.487	184.0	3.437	136.4	3.396	89.9	3.356
Case 3	233.0	3.487	185.0	3.439	137.6	3.398	90.9	3.358

The estimated heat needed for the reboiler at the different loads studied, assuming that the power plant is only producing electricity and no district heat, is in the range of 0.55-1.19 $MW_{thermal}/MW_{el}$. This is in line with what can be found in the literature [35], however, the calculated values for NJV are slightly lower. This is because the energy demand presented in the literature includes energy needed for other process components such as pumps and cooling equipment.

6.2 Scenario 2 – Peak demand

Figure 6-2 shows the results from cases 1 and 2 when steam flow to the reboiler is reduced by 10%. The step reduction in steam flow starts after the model has been simulated for 5000 seconds (around 83 minutes), that is long enough for the system to reached steady state.

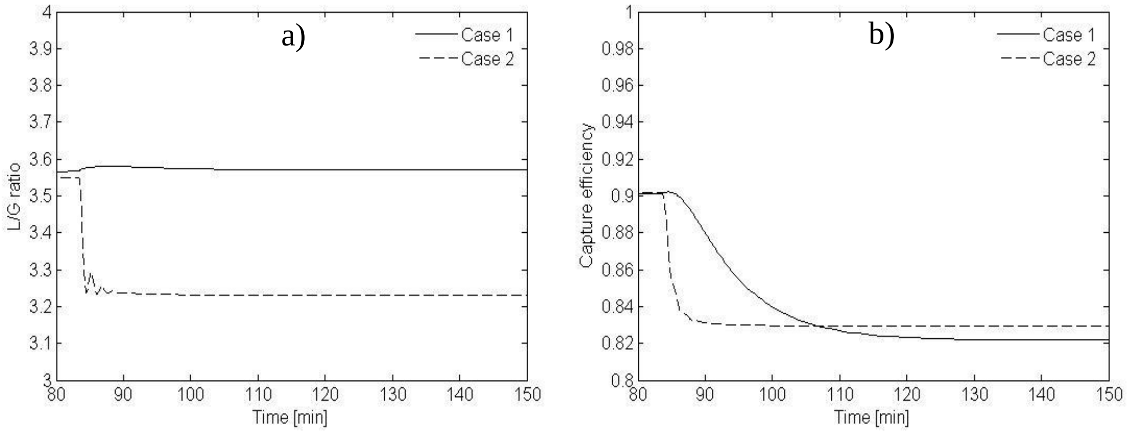

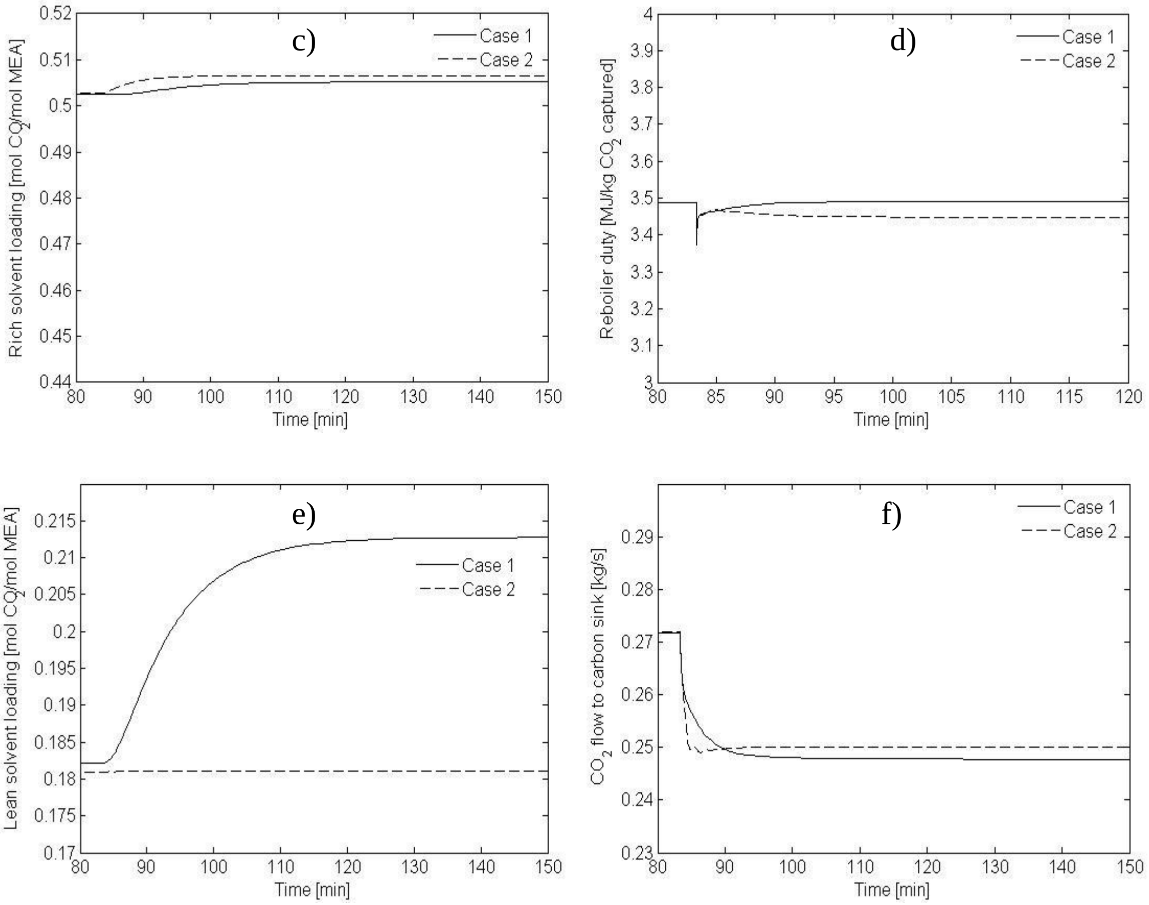

Figure 6-2: Effect of 10% steam reduction for case 1 and 2.

From Figure a) it can be observed that less solvent is needed in case 2 to keep the lean loading at the same level as before. As a result the L/G ratio decreases by 9% when the steam flow is reduced. This means that in case 1, larger flow of solvent is circulated in the system than needed. A minor fluctuation is observed in case 2 due to the controller response. Figure b) shows that the capture efficiency decreases in both cases. In case 1 it is due to the increase in lean loading which means that the solvent entering the absorber can absorb less CO_2. In case 2 the decrease is due to the decreasing L/G ratio, however if the solvent flow is increased, it is not possible to control the lean loading which means that the results would be the same as for case 1 and therefore the efficiency would not increase. It can be observed that the curve is much steeper in case 2 due to controller action.

The steam reduction has little effect on the rich loading and reboiler duty in both cases; see Figures c) and d). A very steep decrease is observed in the reboiler duty, compared to other variables, directly after the negative step change in steam flow is applied. This is due to the direct influence of steam flow on the reboiler duty. The lean loading in case 1, Figure e), increases by 17% after the steam reduction because the rich solvent loading changes little and less energy is provided to the desorber, thus less CO_2 is separated from the solvent. As expected, reduced amount of steam results in less CO_2 separated from the flue gas, see Figure f). The two cases show similar results, however in case 2 more CO_2 is captured due to the lower reboiler duty and higher capture efficiency.

The overall results of steam reduction by 10%, 30% and 50% are presented in Table 6-3. The same figures for the 30% and 50% steam reduction as for the 10% case can be observed in Appendix B. The results are similar to the 10% steam reduction case, however larger variations are observed at larger steam reductions and also larger fluctuations due to controller response. In case 1 the time it takes for the system to reach steady state increases when the steam is further reduced, or from 15 to 60 minutes. In case 2 however the difference observed is not considerable. It can be seen from the table that the system response is around 20 seconds, although it takes longer for some of the variables to start responding to the steam reduction. The rise time is higher in case 1 than in case 2 for all the variables except the rich solvent loading, and increases with increased steam reduction.

Table 6-3: Main results from all steam reductions.

Variable	**Case**	**Response time (seconds)**	**Rise time (minutes)**			**Change (%)**		
Steam reduction			**10 %**	**30 %**	**50 %**	**10 %**	**30 %**	**50 %**
L/G ratio	1	20	1	1	1	+ 0.5	+ 1	+ 1
	2	20	1	1	1	- 9	- 27	- 45
Lean solvent loading	1	30	22	22	24	+ 17	+ 50	+ 84
	2	-	-	-	-	-	-	-
Capture efficiency	1	23	23	23	25	- 9	- 27	- 46
	2	27	3	3	3	- 8	- 26	- 40
Rich solvent loading	1	55	20	20	20	+ 0.5	+ 0.7	+ 1
	2	40	9	11	15	+ 1	+ 1	+ 1
Reboiler duty	1	20	12	31	37	+ 0.1	+ 2	+ 4
	2	20	7	7	7	- 1	- 2	- 3
CO_2 flow to carbon sink	1	20	6	9	12	- 9	- 28	- 47
	2	20	1	1	1	- 8	- 26	- 44

6.2.1 Discussion

The results presented above comply with the findings of Ziaii et al. [15], where effects of reduced steam flow to a stand-alone desorber are studied. From the results it is observed that controlling the lean loading results in a better system performance than if no control strategy is applied, that is, higher capture efficiency and lower reboiler duty, during transition and at the new steady state. The steam reduction causes little fluctuations in the variables studied and the curves are generally rather smooth, with little overshoots. As for scenario 1, the overshoots could be minimized by further tuning of the controllers and a slower steam reduction would make the curves even smoother.

The same calculations are performed to estimate the heat demand of the reboiler as done in scenario 1. The results from these calculations are presented in Table 6-4 and show that the magnitude of the heat demand in both cases is similar, however, the demand is lower in case 2. The difference between the two cases increases with further steam reduction.

Table 6-4: Roughly estimated heat demand of the capture process in Scenario 2 when applied to NJV.

Steam reduction	**0%**		**10%**		**30%**		**50%**	
	MW	MJ/kg CO_2	MW	MJ/kg CO_2	MW	MJ/kg CO_2	MW	MJ/kg CO_2
Case 1	233.9	3.489	213.4	3.492	172.0	3.545	130.1	3.630
Case 2	233.9	3.489	212.8	3.449	170.0	3.409	126.4	3.379

Although case 2 is a better option, the system performance gets poorer in both cases when the steam available decreases. It is however possible to continue running the capture process and maintain high efficiency although less steam is available. This can be done by using lean and rich solvent storage tanks [30]. Such system would start to operate when less steam is available for the capture process. In short, lean solvent is injected to the system and rich solvent is stored until enough steam is available for regeneration. The capture process would therefore have to be designed to handle the increased amount of rich solvent at certain times [16]. A simple flow diagram of a system equipped with such tanks can be seen in Figure 6-3.

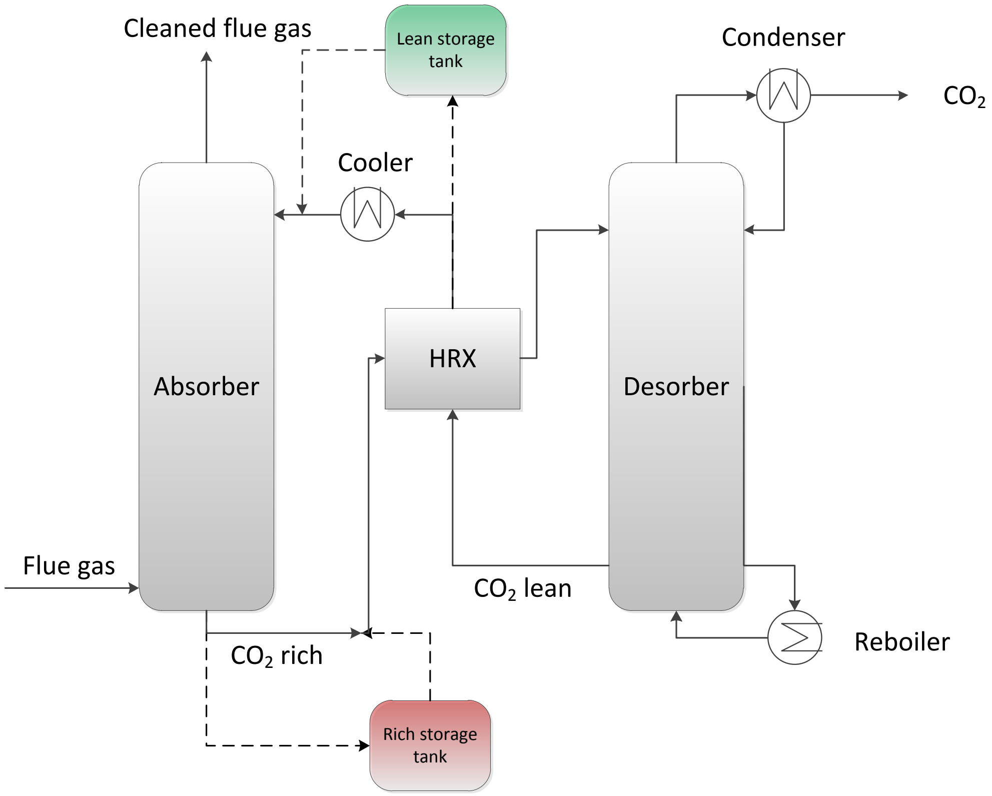
Cleaned flue gas
Lean storage tank
Condenser
CO_2
Cooler
HRX
Absorber
Desorber
Flue gas
CO_2 lean
CO_2 rich
Reboiler
Rich storage tank

Figure 6-3: A simple flow diagram of a chemical absorption process with rich and lean solvent storage tanks.

7 Conclusions

This thesis presents a study of the transient behaviour of post-combustion CO_2 capture with MEA. The thesis contributes to the development of a dynamic post-combustion model by constructing a reboiler model that makes interactions with a steam cycle model possible and by implementing control strategies to control important variables. It is investigated how the capture process responds to load variations and how long it takes for the system to reach steady state. The model developed gives a good understanding of the dynamic behaviour of the capture process and the results are in line with the previous work.

In this work, a reboiler model which makes a connection to a steam cycle possible is constructed. The heat demand of the reboiler can either be controlled by controlling the amount of steam entering the reboiler or the amount of condensate exiting. It is shown that the former control approach has faster dynamic responses and is therefore favoured over the latter approach when investigating the effects of part load operation. A component test shows that the condensate level within the reboiler has an effect on the heat transferred from the steam side to the solution side of the reboiler. In order to investigate the effect of load changes, several closed loop controllers are developed for the absorption process. Controllers for capture efficiency, L/G ratio and lean solvent loading are developed to maintain a good system performance.

Results from load variations show that implementation of control strategies lowers the heat demand of the process considerably and this becomes clearer with larger load variations. It is also shown that the liquid-to-gas (L/G) ratio is more important than the actual flow rates for maintaining the desired capture efficiency when the size of the system is not limiting the process. It takes the system longer time to reach steady state when no control strategies are applied and even longer with larger load variations, or 60 minutes at most. It takes the system around 20 seconds to respond to the load variations in all cases studied. The responses are generally smooth, that is with little or no fluctuations and small overshoots. The relatively fast system response and the smooth transition which can be attained would most likely facilitate integration with a power plant and a CO_2 transport network.

8 Future work

Although it is important to investigate the transient behaviour of the capture process itself, a combined model of the capture process and the connected processes is needed to investigate how the processes will interact. Also a model of the process which handles start-up, shut-down and other disturbances is still required in order to investigate the dynamic behaviour of the system. A model of a power plant and a CO_2 pipe line in Dymola are currently not available to the authors and modelling of those processes does not fit into the time frame of this thesis. However Dymola makes it possible to connect those different processes together and therefore the model developed in this thesis could be a part of a bigger model in the future.

It is also possible to develop and investigate other scenarios of load changes such as one that assures a given capture efficiency or a certain CO_2 emission limit over a given time period with variations in steam availability and flue gas flow to the system. In addition, it could be of interest to develop the post-combustion model used in this thesis and take for example into account reaction kinetic and see how it affects the results.

9 References

[1] Institute for Energy Research Available at:- http://www.instituteforenergyresearch.org/energy-overview/fossil-fuels /(accessed March 27th 2012)

[2] IPCC - Intergovernmental Panel on Climate Change. 2005. *Carbon Dioxide Capture and Storage*. Cambridge, University Press.

[3] Lin, Y.J. [et al.]. 2011. *Plantwide Control of CO_2 Capture by Absorption and Stripping Using Monoethanolamine Solution.* American Control Conference 5067-5072.

[4] Faber, R. [et al.]. 2011. *Open-loop step responses for the MEA post-combustion capture process: Experimental results from the Esbjerg pilot plant*. Energy Procedia 4, 1427-1434.

[5] Polasek, J. and Bullin, J.A. 1984. *Selecting Amines for Sweetening Units*. Energy Progress, September, 146-150.

[6] Freguia, S. And Rochelle, G.T. 2003. *Modeling of CO_2 Capture by Aqueous Monoethanolamine.* The University of Texas at Austin, AIChE Journal.

[7] Åkesson, J. [et al.]. 2011. *Models of a post-combustion absorption unit for simulation, optimization and non-linear model predictive control schemes*. Modelica Conference, Germany.

[8] Pelligini, G. [et al.]. 2009. *Comparative study of chemical absorbents in postcombustion CO2 capture*. Department of Energy Engineering, University of Florens, Italy.

[9] Yang, Y. and Zhai, Rongrong. 2009. *MEA-based CO2 capture technology and its application in power plants*. North China Electric Power University, China.

[10] Wang, M. [et al.]. 2011. *Post-combustion CO2 capture with chemical absorption: A state-of-the-art review*. Chemical Engineering Research and Design 89, 1609-1624.

[11] Taylor, R., & Krishna, R. (1993). *Multicomponent mass transfer*. NewYork: Wiley.

[12] Lawal, A. [et al.]. 2009. *Dynamic modelling of CO_2 absorption for post combustion capture in coal-fired power plants.* Fuel 88, 2455-2462.

[13] Kvamsdal, H.M [et al.]. 2009. *Dynamic modeling and simulation of CO_2 absorber column for post-combustion CO_2 capture*. Chemical Engineering and Processing 48, 135-144

[14] Lawal, A., Wang, M., Stephenson, P., Yeung, H., 2009b. *Dynamic modeling and simulation of CO_2 chemical absorption process for coal-fired power plants*. Comput. Aided Chem. Eng. 27,1725–1730.

[15] Ziaii, S., Rochelle, G.T., Edgar, T.F., 2009. *Dynamic modelling to minimise the energy use for CO_2 capture in power plant aqueous monoethanolamine.* Ind. Eng. Chem. Res. 48, 6105–6111.

[16] Lawal, A. [et al.]. 2010. *Dynamic modelling and analysis of post-combustion CO_2 chemical absorption process for coal-fired power plants.* Fuel 89, 2791-2801.

[17] Vuorinen, A. 2009. *Planning of Optimal Power Systems.* Ekoenergo, 2008.

[18] Onda K, Takeuchi H, Okumoto Y. 1986. *Mass transfer coefficients between gas and liquid packed columns.* J Chem Eng Jpn;1 (1):56-62

[19] Dang, H. and Rochelle, G.T. 2001. *CO_2 Absorption Rate and Solubility in Monoethanolamine/Piperazine/Water*. National Conference on Carbon Sequestration.

[20] Böttinger W. 2005. *NMR-spektroskopische Untersuchung der Reaktivabsorption von Kohlendioxid in wässringen Aminlösunge*. Dissertation. Universität Stuttgart.

[21] Cohen, S.M. [et al.]. 2010. *Turning CO_2 Capture On and Off in Response to Electric Grid Demand: A Baseline Analysis of Economics and Emissions*. Journal of Energy Resources Technology 132, 021003-1 – 021003-8.

[22] VDI Heat Atlas. 2010. *Film wise Condensation of Pure Vapours.* Equation 43. 2nd ed., Springer Berlin Heidelberg, Germany.

[23] Holman, J.P. 2010. *Heat Transfer*. 10th edition, McGraw-Hill, New York.

[24] VDI Heat Atlas. 2010. *Heat Transfer in Pipe Flows*. Equations 26-27. 2nd ed., Springer Berlin Heidelberg, Germany.

[25] Visioli, A. 2006. *Practical PID Control*. Springer-Verlag London Limited 2006.

[26] Ahlgreb, Roy. 2001. *What they are, what they do: A steam trap primer*. Ashrae Journal 43, 36-39.

[27] Kenig, E.Y., Schneider, R., Górak, A., 2001. *Reactive absorption: optimal process design via optimal modelling*. Chem. Eng.Technol. 56, 343–350.

[28] Kvamsdal, H.M. and Rochelle, G.T. 2008. *Effects of the Temperature Bulge in CO_2 Absorption from Flue Gas by Aqueous Monoethanolamine*. Ind. Eng. Chem. Red, 47, 867-875.

[29] Joseph, G.T and Beachler, D.S. 1998. *Scrubber Systems Operation Review.* Self-Instructional Manual. Second Edition. Environmental Programs, North Carolina State University. 11-25 – 11-29.

[30] Haines, and M.R, Davison, J.E. 2009. *Designing Carbon Capture power plants to assist in meeting peak power demand.* Energy Procedia 1, 1457-1464.

[31] Colonna, P. and van Putten, H. 2007. *Dynamic modeling of steam power cycles: Part II – Simulation of a small simple Rankine cycle system.* Applied Thermal Engineering 27, 2566-2582.

[32] Davis, J. and Rochelle, G. 2009. *Thermal degradation of monoethanolamine at stripper conditions*. Energy Procedia 1, 327-333.

[33] Dassault Systems. Available at:- http://www.3ds.com/ (accessed May 24th 2012)

[34] Modelica. Available at:- https://modelica.org/ (accessed May 24th 2012)

[35] Ali, C. 2004. *Simulation and optimization of a coal-fired power plant with integrated CO_2 capture using MEA scrubbing*. Master Thesis, University de Waterloo.

10 Appendix A – Scenario 1

10.1 Load reduction from full load down to 60% load

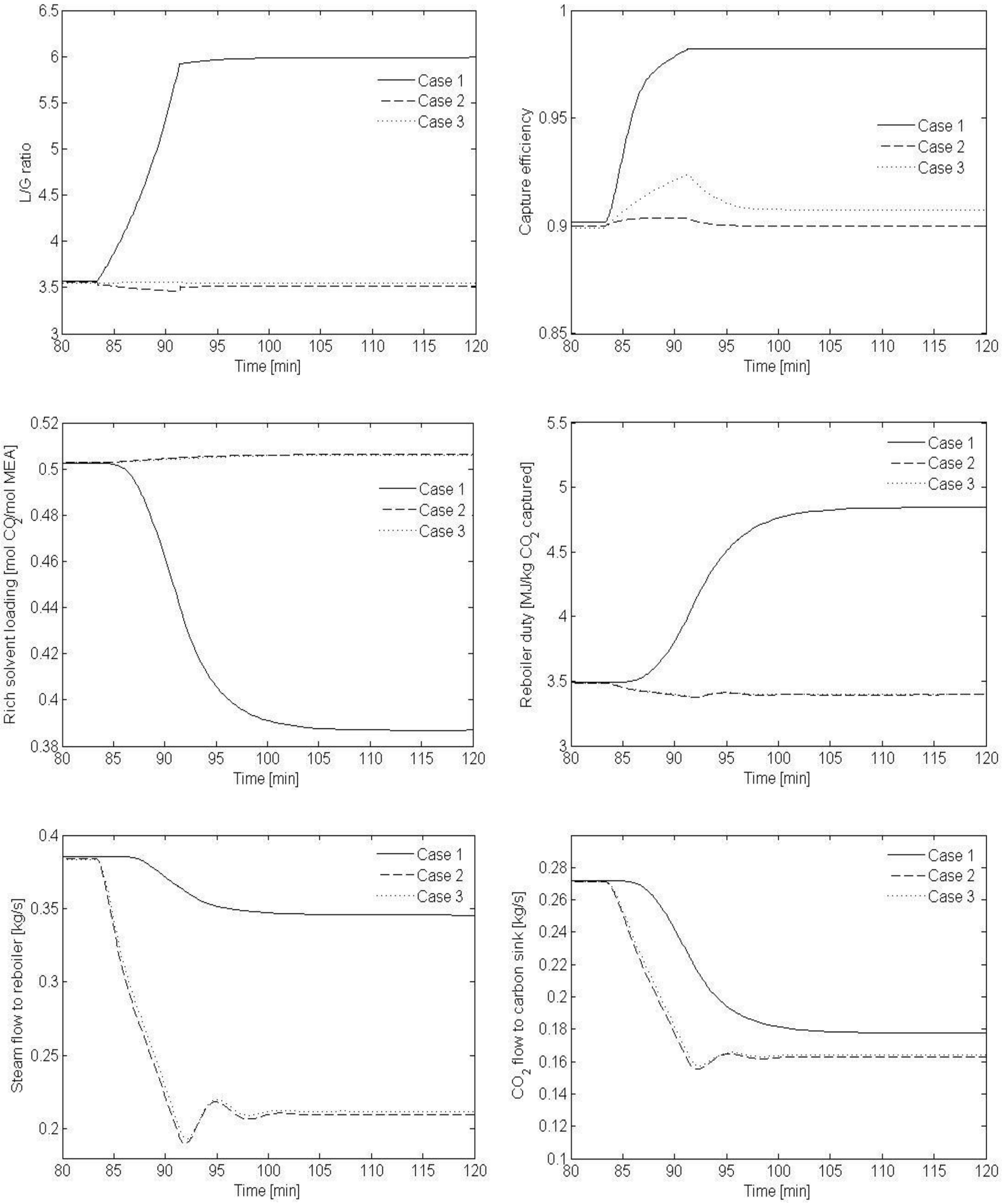

Figure 10-1: Effect of load reduction from 100% to 60% load for case 1, 2 and 3.

10.2 Load reduction from full load down to 40% load

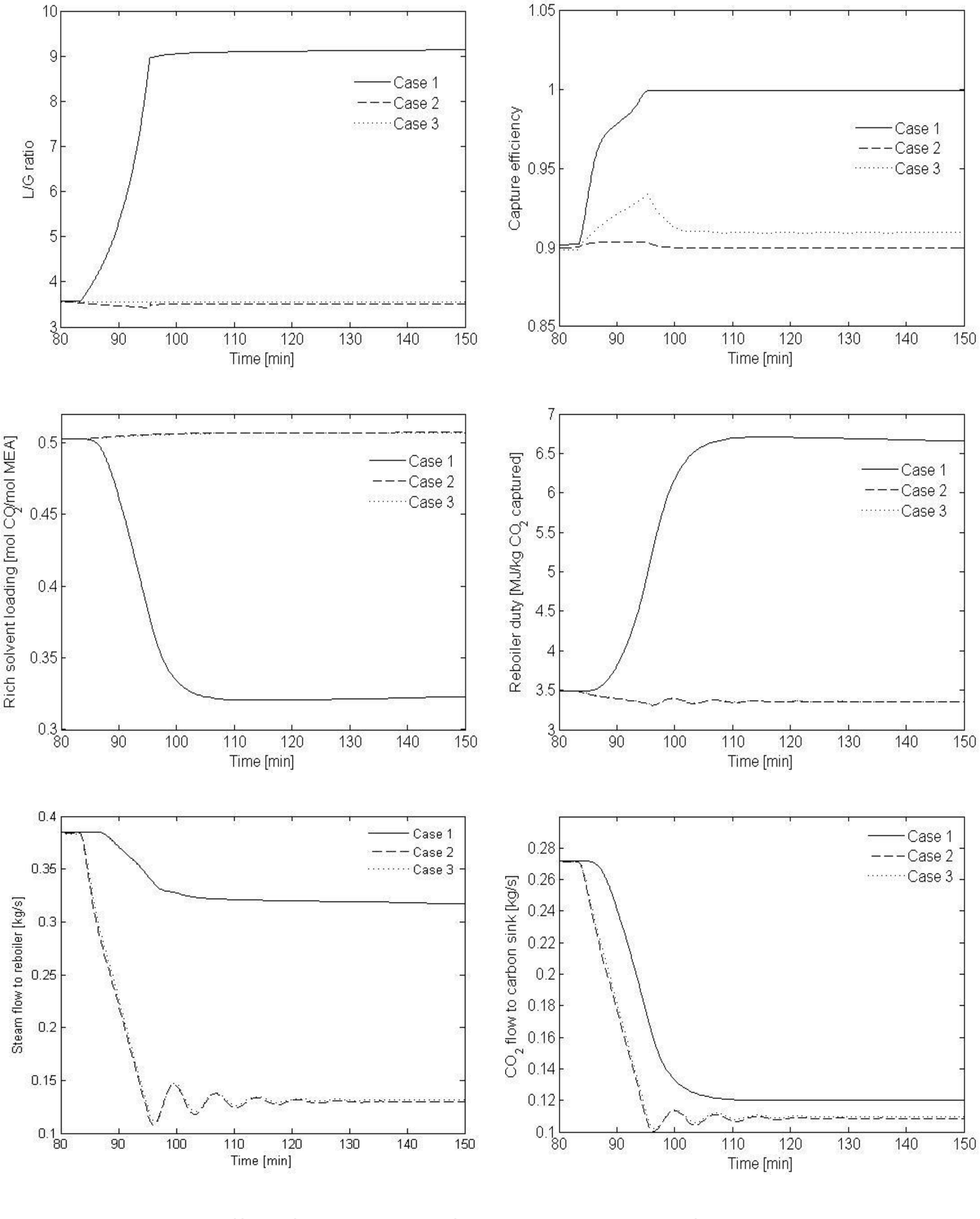

Figure 10-2: Effect of load reduction from 100% to 40% load for case 1, 2 and 3.

11 Appendix B – Scenario 2

11.1 Steam flow reduction of 30%

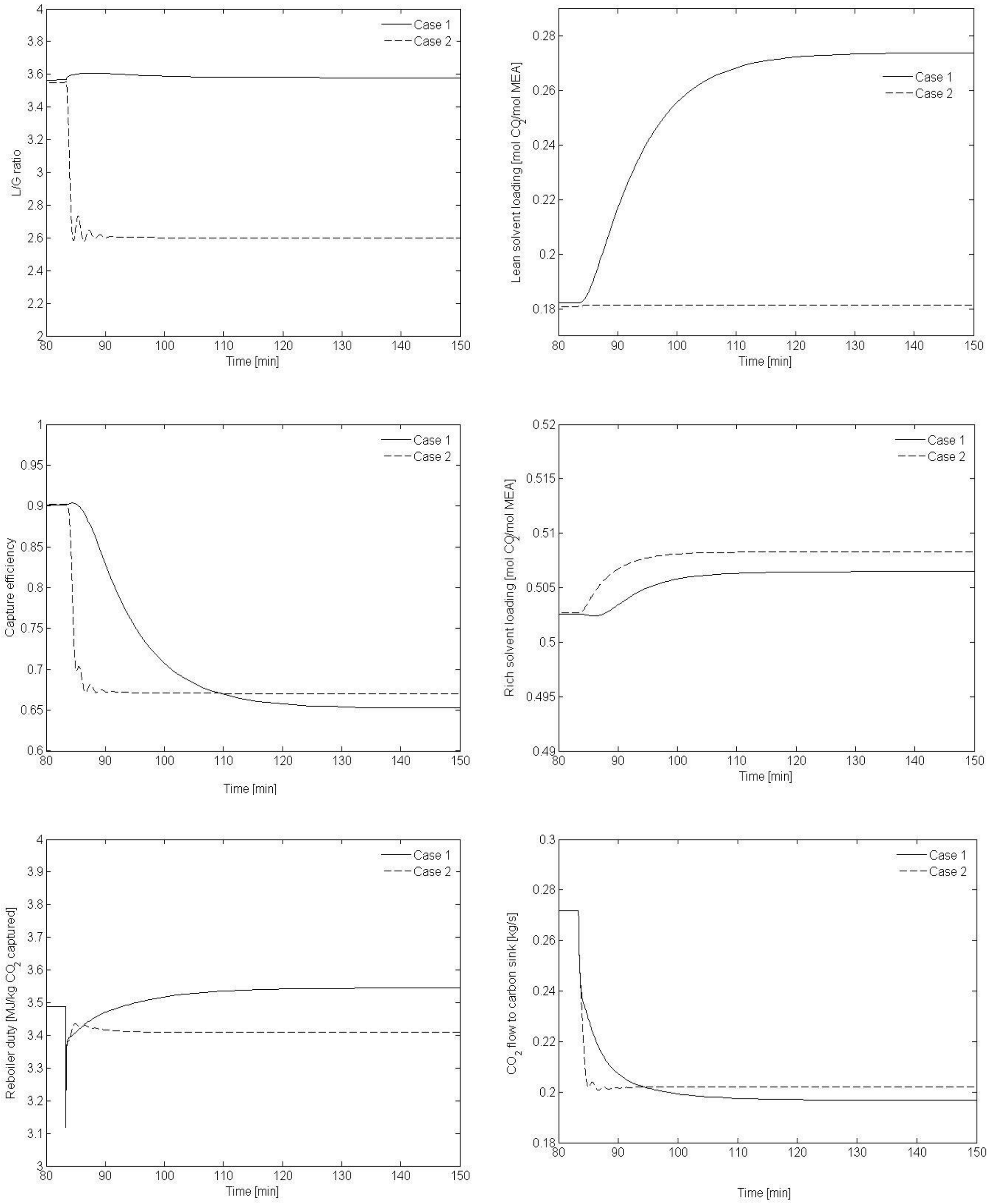

Figure 11-1: Effect of 30% steam reduction for case 1 and 2.

11.2 Steam flow reduction of 50%

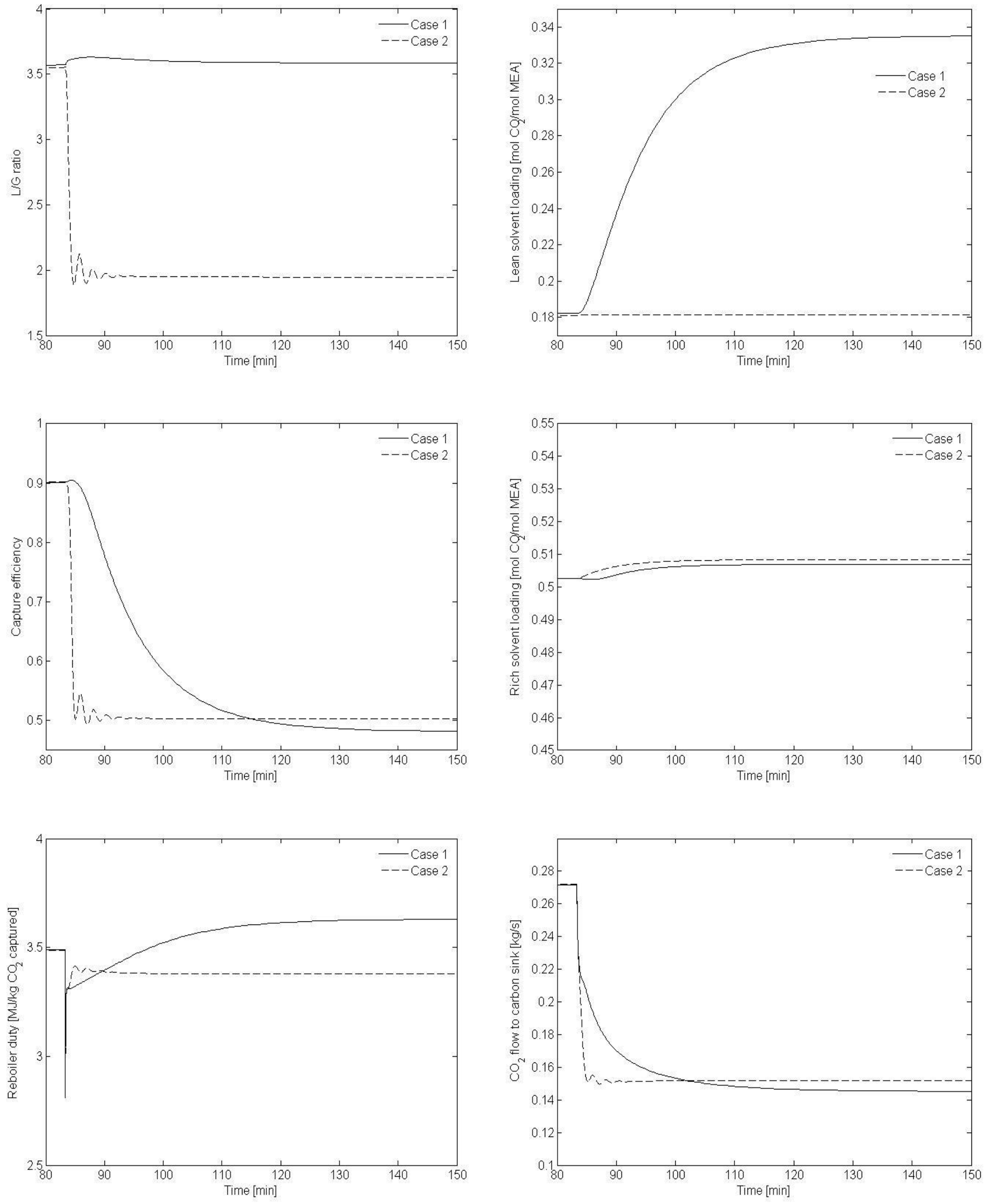

Figure 11-2: Effect of 50% steam reduction for case 1 and 2.